

Integrated Masters in Chemical Engineering

*Photocatalytic production of  
hydrogen from biomass*

**Master's Thesis**

by

**Liliana Angélica da Silva Ferreira**

Developed within the scope of Dissertation subject

Performed at

**LCM - Laboratory of Catalysis and Materials  
Associate Laboratory LSRE-LCM**



Supervisor: Dr. Cláudia Sofia Castro Gomes da Silva

Co-Supervisor: Prof. Joaquim Luís Bernardes Martins de Faria



**Chemical Engineering Department**

July 2014







## Agradecimentos

A realização deste trabalho só foi possível com a contribuição de algumas pessoas a quem gostaria de agradecer.

Em primeiro lugar, ao Professor Joaquim Faria por me ter dado esta oportunidade de investigar nesta área para a qual o seu contributo como professor e agora como co-orientador ajudou a fomentar o meu gosto pela mesma assim como agradeço pela disponibilização do material e espaço do qual é responsável.

À minha orientadora, a Doutora Cláudia Silva, pelo empenho e preocupação para com o meu trabalho, pela partilha de conhecimentos na área de investigação. Gostaria de agradecer também por todo o apoio dado em termos pessoais e os quais foram fulcrais para a realização desta tese.

Ao Professor Doutor José Luís Figueiredo por ter disponibilizado todos os recursos técnicos do Laboratório de Catálise e de Materiais do qual é diretor.

A todos os meus colegas de laboratório, em especial: Tânia Silva, Teresa Pinho, Cátia Freitas, Patrícia Ramalho, Inês Rocha, Ricardo Segundo e ainda: Salomé Soares, Sérgio Torres, Luísa Pastrana, Alexandra Gonçalves, Nuno Moreira e Carla Esteves entre outros.

Agradeço ainda a outros, por me acompanharem nestes anos: Ana Campos, Gisela Lima, Joana Leão Pereira, Diana Medeiros e Elson Gomes. Um obrigado também ao Tiago Torres pelo apoio e amizade nestes meses.

Para finalizar como não poderia deixar de ser agradeço aos meus pais, Alzira e Eduardo, avós, Marcela e Adélio e tios/padrinhos, Angélica e José por terem sempre acreditado em mim e estarem comigo nos momentos mais complicados. A eles um enorme obrigada por tudo, sempre!

---

## Abstract

Hydrogen is a gas widely used in the chemical industry. Since its energy potential was discovered, the research around this molecule has been mostly focused on this subject. With the increase of the demand for energy the interest on finding alternative routes for obtaining hydrogen has been growing. Hydrogen is considered as an alternative to fossil fuel derivatives, because of the possibility of using it in fuel cells for electrical energy production. Currently H<sub>2</sub> is mostly produced from hydrocarbon materials, which brings environmental problems associated. There is an increasing interest on finding alternative and clean routes for hydrogen production. Heterogeneous photocatalytic processes, based on the use of semiconductor nanoparticles as photocatalysts, have been gaining increasing commercial interest worldwide, mostly due to the possibility of using sunlight as irradiation source. Taking these factors into account, the aim of this work is to study the photocatalytic hydrogen production from biomass. Photocatalytic reforming of biomass-containing waters is an efficient method for the production of hydrogen. Moreover, since that the sacrificial reagent used is biomass, an economical value is added to something that is often considered waste and/or has low commercial value.

In photocatalysis field titanium dioxide (TiO<sub>2</sub>) has been widely used as a catalyst because of its semiconducting properties, and high stability and efficiency under UV irradiation. However, the addition of co-catalyst, which is usually a noble metal such as platinum, gold, iridium or palladium is required for efficient hydrogen evolution. Moreover, the introduction of a carbon phase such as carbon nanotubes (CNTs) normally leads to an increase in the efficiency of hybrid CNT-TiO<sub>2</sub> photocatalysts. The effect of the CNT-TiO<sub>2</sub> preparation method and of the type of metal co-catalyst, as well as the thermal conditions used for the reduction of the metal particles, on the efficiency of H<sub>2</sub> generation from methanol-water solutions has been assessed. The type of biomass used as sacrificial reagent in the photocatalytic reaction was also studied, the attention being focused on saccharides namely glucose, arabinose, fructose, and cellobiose.

It was concluded that hybrid CNT-TiO<sub>2</sub> catalysts impregnated with platinum nanoparticles promote the generation of higher amounts of hydrogen. Among the biomass compounds tested, glucose revealed to be the most efficient sacrificial reagent for the photocatalytic reforming process.

Other properties, and variables could be studied in order to optimize the process of hydrogen production. Some suggestions for a future work are presented.

---

**Keywords:** photocatalysis, Hydrogen production, titanium dioxide, noble metals, hybrid materials, titania catalysts, biomass reforming.

---

## Resumo

O hidrogénio ( $H_2$ ) é um gás que tem vindo a ser amplamente utilizado na indústria química. Desde que foi conhecido o seu potencial energético, os trabalhos de investigação em torno desta molécula têm-se centrado maioritariamente nesse tema.

O aumento das necessidades energéticas tem conduzido a uma procura por métodos alternativos de produção de hidrogénio. Este gás é considerado uma alternativa aos derivados de combustíveis fósseis devido à possibilidade de ser utilizado em células combustíveis.

Grande parte do hidrogénio é obtido a partir de hidrocarbonetos, o que acarreta problemas ambientais, daí o interesse em investigar processos alternativos mais limpos.

Os processos fotocatalíticos heterogêneos, baseados no uso de nanopartículas semicondutoras, têm vindo a ganhar maior interesse a nível comercial sobretudo pela possibilidade de usar energia solar como fonte de irradiação.

Tendo em conta estes fatores, neste trabalho pretende-se estudar a produção fotocatalítica de hidrogénio a partir de biomassa. O *reforming* fotocatalítico de compostos derivados de biomassa é um método eficiente para a produção de hidrogénio. Além das vantagens de ser um processo fotocatalítico, o facto de se utilizar biomassa como reagente de sacrifício é um fator interessante tendo em conta que é adicionado um valor comercial a algo que é muitas vezes considerado desperdício ou que tem valor comercial residual.

O dióxido de titânio ( $TiO_2$ ) é o catalisador mais usado em processos fotocatalíticos devido às suas propriedades semicondutoras e à sua alta estabilidade e eficiência sob irradiação UV. Contudo, para que haja uma produção eficiente de hidrogénio, é necessária a adição de um cocatalisador, normalmente um metal nobre como a platina, o ouro, o paládio ou o irídio. A introdução de uma fase de carbono, por exemplo de nanotubos de carbono (CNTs) conduz normalmente à formação de materiais híbridos de CNT- $TiO_2$  com elevada eficiência fotocatalítica. Neste trabalho foi estudado o efeito do método de preparação destes materiais híbridos de CNT- $TiO_2$  assim como do tipo de cocatalisador e da sua temperatura de redução na eficiência de produção de  $H_2$  a partir de misturas de metanol-água. O tipo de biomassa utilizada como reagente sacrifício na reação fotocatalítica foi também estudado, tendo sido focada a atenção em sacarídeos nomeadamente a glicose, arabinose, frutose e celobiose.

Com os estudos realizados concluiu-se que os materiais híbridos CNT- $TiO_2$  nos quais foram introduzidas partículas de platina na superfície promovem a geração de maiores quantidades de hidrogénio. Das fontes de biomassa testadas, a glicose foi a que apresentou melhores resultados como reagente sacrifício para o processo de *reforming* fotocatalítico.

---

Outras propriedades assim como outras variáveis podem ainda ser estudadas com o objetivo de otimizar o processo de produção de hidrogénio. Algumas sugestões de trabalho futuro são apresentadas.

**Palavras Chave :** fotocatalise, produção de hidrogénio, dióxido de titânio, metais nobres, materiais híbridos, catalisadores de titânio, *reforming* de biomassa.

---



## Declaração

Declara, sob compromisso de honra, que este trabalho é original e que todas as contribuições não originais foram devidamente referenciadas com identificação da fonte.

---

*Liliana Angélica da Silva Ferreira*

*Porto, 04 de Julho de 2014*

---

---

# Index

<b>1</b>	<b>Introduction.....</b>	<b>1</b>
1.1	Background and Relevance.....	1
1.2	Objectives .....	5
1.3	Dissertation outline.....	5
<b>2</b>	<b>State of the Art.....</b>	<b>7</b>
2.1	Hydrogen .....	7
2.2	Photocatalysis .....	8
2.3	Biomass .....	10
<b>3</b>	<b>Materials and Methods .....</b>	<b>12</b>
3.1	Catalysts synthesis.....	12
3.2	Catalysts characterization.....	12
3.3	Photocatalytic reactions.....	13
<b>4</b>	<b>Results and discussion .....</b>	<b>15</b>
4.1	Catalysts characterization.....	15
4.2	Photocatalytic results.....	21
4.2.1	Photocatalytic hydrogen generation from methanol .....	21
4.2.2	Photocatalytic hydrogen generation from saccharides.....	25
<b>5</b>	<b>Conclusions.....</b>	<b>29</b>
5.1	Accomplished Objectives .....	29
5.2	Limitations and future work .....	29
5.3	Final Appreciation .....	30
<b>6</b>	<b>References .....</b>	<b>31</b>
Appendix A	Characterization .....	35
Appendix B	Results.....	38

## List of figures

<i>Figure 1. Schematic Mechanism of photocatalytic hydrogen production from biomass in a semiconductor (SC) catalyst and a metal (M) co-catalyst. M represents metal loaded in the catalyst that could be Pt for example.....</i>	<i>3</i>
<i>Figure 2. Schematic representation of reaction setup. ....</i>	<i>14</i>
<i>Figure 3. XRD patterns of TiO<sub>2</sub> (a), 1%Pt/TiO<sub>2</sub> (b), (CNT-TiO<sub>2</sub>)<sub>ox</sub> (c) and 1%Pt/(CNT-TiO<sub>2</sub>)<sub>ox</sub> (d). ....</i>	<i>15</i>
<i>Figure 4. SEM images of TiO<sub>2</sub> (a) and composite (CNT-TiO<sub>2</sub>)<sub>ox</sub> (b), and TEM images of 1% Pt/ TiO<sub>2</sub> (c) and (d), and 1 % Pt/(CNT- TiO<sub>2</sub>)<sub>ox</sub> (e) and (f). EDX spectrum obtained from analysis of the 1% Pt/(CNT-TiO<sub>2</sub>)<sub>ox</sub> catalyst in zone Z1 (see Appendix A)(g).....</i>	<i>18</i>
<i>Figure 5. Attenuated Total Reflectance (ATR) spectra of TiO<sub>2</sub>, CNTox-TiO<sub>2</sub> and (CNT-TiO<sub>2</sub>)<sub>ox</sub>.....</i>	<i>19</i>
<i>Figure 6. Diffused reflectance UV-Vis. (DR-UV Vis.) spectra of different catalysts: TiO<sub>2</sub> (a) and (CNT-TiO<sub>2</sub>)<sub>ox</sub> (b) with different metals loaded. ....</i>	<i>20</i>
<i>Figure 7. Hydrogen production (cumulative) (a) and profiles (b) using different catalysts with loaded with 1% Pt in a 10% vol. methanol aqueous solution.....</i>	<i>22</i>
<i>Figure 8. TPR for co-catalysts: Pt(blue), Pd (red), Au (violet) and Ir (green).....</i>	<i>23</i>
<i>Figure 9. cumulative production of hydrogen and total amount of hydrogen produced respectively during 120 minutes for catalysts treated at 200°C (a), (c) and at 400°C (b), (d) in 10 % Methanol solution.....</i>	<i>24</i>
<i>Figure 10. Saccharides molecular structure and respective molecular formula.....</i>	<i>25</i>
<i>Figure 11. Evolution and production respectively of Hydrogen with glucose (a),(b); cellobiose (c),(d); arabinose (e),(f) and fructose (g),(h). Total amount of hydrogen produced with 1%Pt/TiO<sub>2</sub> and 1%PT/(CNT-TiO<sub>2</sub>)<sub>ox</sub> for different saccharides solution (i). ....</i>	<i>27</i>
<i>Figure 12. Isotherms for TiO<sub>2</sub> (a), CNTs(b) and (CNT-TiO<sub>2</sub>)<sub>ox</sub>. ....</i>	<i>36</i>
<i>Figure 13. Z1 of 1% Pt/(CNT-TiO<sub>2</sub>)<sub>ox</sub> where was analysed the EDXS spectra. ....</i>	<i>37</i>
<i>Figure 14. Evolution of hydrogen production for catalysts treated at 200°C (a) and at 400°C (b). ....</i>	<i>39</i>

# List of Tables

*Table 1. BET surface area ( $S_{BET}$ ), and anatase ( $x_{anatase}$ ) and carbon ( $C_{TG}$ ) contents of the used materials.*  
..... 16

# Nomenclature and Glossary

## *Roman letters*

$S_{\text{BET}}$  Specific Surface Area  $\text{m}^2 \text{g}^{-1}$

## *Greek letters*

$\lambda$  Wavelength Nm

## *Acronym list*

ATR	Attenuated Total Reflectance
BET	Brunauer-Emmett-Teller
CB	Conduction Band
CEMUP	Centro de Materiais da Universidade do Porto
CNT	Carbon Nanotubes
DR UV-Vis	Diffuse Reflectance Ultraviolet-Visible
DRIFT	Diffuse Reflectance Infrared Fourier Transformed
EDXS	Energy-Dispersive X-Ray Spectrometric Analysis
KM	Kubelka-Munk
LPG	Liquefied Petroleum Gas
MWCNT	Multi-Walled Carbon Nanotubes
SEM	Scanning Electron Microscopy
SWCNT	Single-Walled Carbon Nanotubes
TEM	Transmission Electron Microscopy
TGA	Thermogravimetric Analysis
TPR	Temperature Programmed Reduction
UV-Vis	Ultraviolet-Visible
VB	Valence Band
XRD	X-ray Diffraction

# 1 Introduction

## 1.1 Background and Relevance

The increase of environmental concerns associated to the high demand of energy observed in the past decades, mostly due to the population growth and technological development, has resulted in a great necessity to find alternative routes for obtaining clean energy sources. The processes currently used to produce energy are mainly based on fossil resources that generate high levels of atmospheric pollution. This atmospheric contamination has a relation with the burn of hydrocarbons that results in emission of greenhouse effect gases such as CO<sub>2</sub>, CH<sub>4</sub> and NO<sub>x</sub>. Due to these factors a great effort have been put on trying to find economically and environmental friendly routes to produce energy. Hydrogen (H<sub>2</sub>) is widely considered as an attractive energy source to replace conventional fossil fuels, both from the environmental and economic standpoints. After Fujishima and Honda in 1970's described a photocatalytic process to obtain hydrogen using TiO<sub>2</sub> as catalyst and a Pt counter electrode [1], the scientific community has devoted a huge interest in producing H<sub>2</sub> by photocatalytic processes.

Hydrogen is a promising source for obtaining energy because of its small dimension and its high energy per unit mass higher than fossil fuels [2]. Another factor is the abundance on earth. Although hydrogen exists in a large scale on earth, this element is usually found in bond form *i.e.* linked to other elements such as water and not as a sole molecule. This may constitute a disadvantage as others such as safety since hydrogen is lighter than air, or the low ignition energy (0.02 mJ) when compared to the fossil fuels (0.29 mJ for methane and 0.24 mJ for gasoline) [2]. On the other hand, when combined with fuel cell technology, it generates carbon free energy, and only water as by-product.

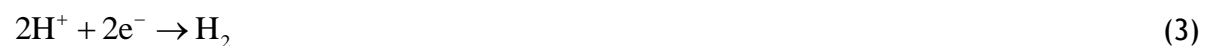
The production of hydrogen by splitting the water molecule can be considered as an ideal route. This may be achieved by electrolysis or by photocatalytic water splitting. While the first process shows the disadvantage of requiring the use of high amounts of electrical energy, the second one has been considered a promising technology, since H<sub>2</sub> production can be driven by solar light. However, the efficiency of this last process remains quite far from the required for applicability. A common strategy usually applied to increase the efficiency of photocatalytic water splitting is by addition of sacrificial reagents, usually alcohols, such as ethanol or methanol [3, 4]. Based in this principle, photocatalytic reforming processes gained importance, since biomass-derived compounds such as saccharides, proteins, phenolics, etc., can be used as sacrificial reagent for producing H<sub>2</sub>. These compounds are usually industrial by-products with low commercial value, and/or wastes. Traditional methods of energetic

valorization of such products are mostly based on thermal treatment at very high temperatures. Nonetheless, there is a great environmental disadvantage on this type of processes for obtaining energy because the pyrolysis of organic matter originates carbon-containing and other toxic gases that are the major responsible for atmospheric pollution.

And it is here that photocatalysis plays an important role. As the name suggests, photocatalysis is a catalysis field, which deals with light-activated reactions. Heterogeneous photocatalysis is a physical-chemical process similar to typical heterogeneous catalysis but using light instead of thermal activation and holding the following components: a reactant, a photon with the adequate energy, and a semiconductor catalyst. Heterogeneous catalytic processes include the following steps: the transfer of the reactants from the bulk to the catalyst surface, adsorption of the reactants followed by reaction on the catalyst surface and desorption of the products. Photocatalytic processes only differ from these steps in the part of reaction at the catalyst surface, which just happens after the absorption of the photons by the semiconductor catalyst, followed by the creation of electron-hole pairs, which dissociate and form photoelectrons and positive holes (electron vacancies). After that, surface reactions happen such as ionosorption, charge neutralization, radical formation, etc [5, 6].

The photocatalytic reaction is initiated by the excitation of the catalyst with light with energy ( $h\nu$ ) equal or higher than the bandgap energy of the semiconductor ( $E_{bg}$ ):  $h\nu \geq E_{bg}$ . When the light irradiates the surface of semiconductor the electrons become excited, being transferred from the valence band ( $VB$ , Highest Occupied Molecular Orbital - HOMO) to the conduction band ( $CB$ , Lowest Unoccupied Molecular Orbital - LUMO), generating electron-hole pairs ( $e^-/h^+$ ), Eq. 1.

In the photocatalytic water splitting process, electrons and holes are involved in redox reactions which will originate  $H_2$  and  $O_2$  as products, as follows [7]:



The overall reaction is:



In the photocatalytic reforming process, the reaction described in Eq. 2 is forced by the introduction of a sacrificial electron donor, as illustrated in Fig 1. Since the objective is the production of  $H_2$ , which is obtained through the water reduction semi-reaction (Eq. 3), the

addition of a sacrificial electron donor that will react with photogenerated holes, will lead to an increase in the photoefficiency of the process. These reducing agents are usually alcohols such as methanol or biomass-derived compounds such as glycerol and saccharides. Biomass is a product that typically have a low economic value and in the major of cases are a surplus from various industries such as food or paper mills [8]. Biomass can be classified in four main categories: i) energy crops (herbaceous energy crops, woody energy crops, industrial crops, agricultural crops and aquatic crops); ii) agricultural residues and waste (crop waste and animal waste); iii) forestry waste and residues (mill wood waste, logging residues, trees and shrub residues); iv) industrial and municipal wastes (municipal solid waste, sewage sludge and industry waste) [9].

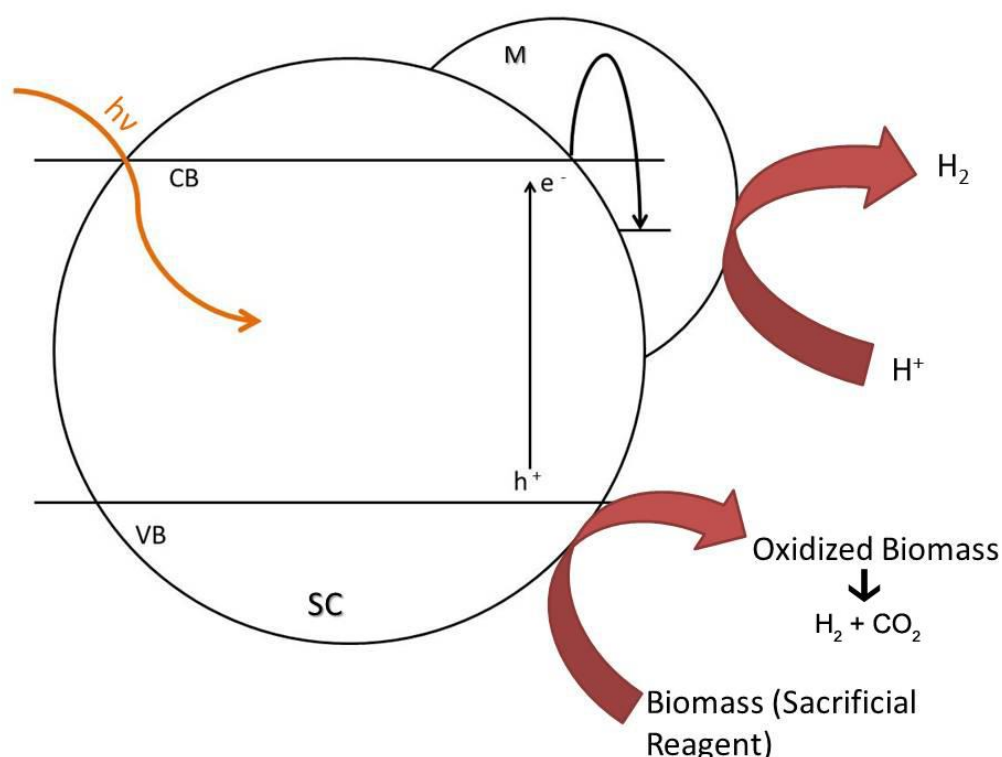
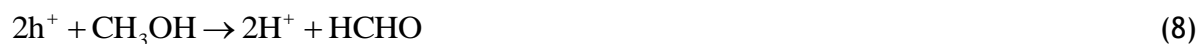


*Figure 1. Schematic Mechanism of photocatalytic hydrogen production from biomass in a semiconductor (SC) catalyst and a metal (M) co-catalyst. M represents metal loaded in the catalyst that could be Pt for example.*

Methanol is often used as organic sacrificial reagent for the photocatalytic  $H_2$  production [4]. In this case, the reactions involved are the following, for this example was used the system of methanol/water [10]:



The overall reaction:



As can be inferred by the reactions described above, when an organic sacrificial reagent is used,  $\text{H}_2$  is not only generated from  $\text{H}^+$ , but also from its degradation, *i.e.*, mineralization into  $\text{CO}_2$  and  $\text{H}_2$ .

Many types of semiconductors can be used as photocatalysts such as metal oxides and sulphides. Titanium dioxide ( $\text{TiO}_2$ ) is the benchmark catalyst in photocatalytic applications, mostly because the relatively high efficiency in producing electron-hole pairs under UV light (the energy irradiated required is a value around 3 eV, that corresponds to  $\cong \lambda < 400\text{nm}$ ) associated to other important factors such the cost and the stability [7].

Nevertheless, undesired recombination of electron-hole pairs is still being the limiting step in photocatalytic processes. One strategy for increasing the photoefficiency of semiconductor catalysts is by loading their surface with metal particles. Noble metal nanoparticles at the surface of the semiconductor work as co-catalysts, acting as electron sinks and inhibiting electron/hole recombination, and also enhancing photo-charge lifetime and electron transfer [4, 11].

The metals with work functions higher than  $\text{TiO}_2$ , *i.e.*, which act as good electron trappers are usually noble metals such as Pt (Platinum), Au (Gold), Pd (Palladium), Ni (Nickel), Cu (Copper), and Ag (Silver) and some transition metals. This type of compounds that do not work as catalyst itself are usually named “co-catalysts” or “enhancers” since they improve the photocatalyst efficiency by creating a synergetic effect.

In order to increase the efficiency of TiO<sub>2</sub>-based photocatalysts some techniques have been proposed. One of them consists in the use of hybrid materials of TiO<sub>2</sub> and carbon nanotubes (CNTs). CNTs were reported by Iijima in 1991 for the first time [12]. Some properties of CNTs turn them as important materials for developing efficient TiO<sub>2</sub>-based catalysts [13]. CNTs have an architecture that facilitates the transfer of charges to/from electrodes (in the case of photo- electrochemical reactions) or improve charge separation in case of photocatalysts, since they have exceptional conductivity properties. The high surface area and the possibility of acting as photosensitizers are also appealing assets for using CNTs in photocatalysis [14]. Since that only a small part from solar spectra is UV light (4~5%), exploring the photosensitizing properties of CNTs could be interesting to widen the light absorption spectrum of TiO<sub>2</sub> [15].

## 1.2 Objectives

The aim of the present work consists in the study of important variables of the photocatalytic hydrogen production from biomass, such as the type of catalyst, co-catalyst, their preparation conditions and type of biomass. Bare TiO<sub>2</sub> and hybrid materials combining TiO<sub>2</sub> with CNTs were used as catalysts and Pt (Platinum), Ir (Iridium), Au (Gold) and Pd (Palladium) as co-catalysts. The influence of preparation conditions such as composite synthesis method, and temperature of calcination/reduction on H<sub>2</sub> production efficiency was assessed. The influence of the nature of the biomass-derived sources, more specifically saccharides (glucose, arabinose, fructose and cellobiose) was also studied. The optimization of the process regarding these variables is the main milestone of this work.

## 1.3 Dissertation outline

The dissertation is organized as follows:

- Chapter 2 contains a description of the state of the art, in which are presented some results and work in the fields of hydrogen production, photocatalysis and biomass processes.
- In Chapter 3 it is described the materials, equipment and methodology used for catalysts synthesis and characterization, and for photocatalytic reactions.
- The Results and Discussion are presented in Section 4, which contains the catalysts characterization and photocatalytic results, including those for the different types of catalysts, the effect of the nature of the co-catalyst and the effect of the type of saccharides in the efficiency of hydrogen production.
- Finally, the conclusions and some suggestions of future work are presented in Section 5.



## 2 State of the Art

The exponential growth of the human population leads to an increase in energy demand. This happens due to industrial, agriculture, transport and service intensification. In all of these fields energy is important since that is transversal to any type of human activity. This can be considered a cycle because with the advance of science, an increase in life quality and life expectancy is predictable. All of these factors result in a growth of the energy demand. Since that a big part of the energy produced in the planet comes from fossil fuels this leads to price speculation and environmental problems. Energy production from fossil fuels has some issues such as the contribution for the increase of greenhouse effect because of the emissions of gases such as carbon oxides and methane to the atmosphere. The search for alternative energy sources is currently one of the most important research topics.

### 2.1 Hydrogen

Hydrogen is the most abundant element on Earth, which is mostly found combined with other elements due to its highly reactivity as a molecule. Some of the compounds where it is most common found this element are hydrocarbons, water and biomass [16]. Currently it is mostly used in chemical industries, but the interest around the energy capacities of this element are growing up [17]. Research on efficient energy production has been increasing with the growing concern about the climate change and environmental issues. The ideal solution consist in the application of cleaner and, when possible, renewable energy. And it is here that hydrogen appears as solution since it can be used in fuel cells, in which energy can be produced without generating hazardous residues, greenhouse gases and other pollutant gases and wastes. In addition, when compared to other known fuels, hydrogen has the highest energy content per mass unit [2]. Unfortunately the industrial methods to obtain hydrogen are yet environmental unfriendly or are economically unviable. This compound could be obtained from several sources such as coal, natural gas, liquefied petroleum gas (LPG), propane, methane ( $\text{CH}_4$ ), gasoline, light diesel, dry biomass, biomass-derived liquid fuels (such as methanol,  $\text{C}_2\text{H}_5\text{OH}$ , biodiesel), as well as from water [18].

Hydrogen production can be driven through two main routes: fuel processing and non-reforming processes [17]. In the fuel processing one can find hydrocarbon processing where hydrocarbon reforming reactions are included such as steam reforming that are currently the most used industrial process to obtain hydrogen, which efficiency can go up to 85% and representing 50% of the production of consumed hydrogen [16]. Other reactions from hydrocarbon reforming group are partial oxidation, autothermal reforming, carbon (coke)

formation, water-gas shift and CO oxidation. From fuel processing, where hydrocarbon reforming is included, there are other ways to obtain hydrogen such as desulfurization, Pyrolysis, Plasma reforming, aqueous phase reforming and Ammonia reforming. Non-reforming hydrogen production include other processes to obtain hydrogen such as hydrogen from biomass (biomass gasification and biological hydrogen) and hydrogen from water (electrolysis, thermochemical water splitting and photoelectrolysis) [19].

## 2.2 Photocatalysis

Defined by IUPAC as *a change in the rate of a chemical reaction or its initiation under the action of ultraviolet, visible or infrared radiation in the presence of a substance—the photocatalyst that absorbs light and is involved in the chemical transformation of the reaction partners*, photocatalysis is currently an important field of heterogeneous catalysis [20].

Various types of reactions could be included in this field such as oxidation-reduction reactions, dehydrogenation, removal of pollutants from water and air, hydrogen and electron transfer and energy production/storage. The reactions could be carried out in various types of media such as gas phase, pure organic liquid phase and/or aqueous solutions [5, 6].

The photocatalytic reactions could be divided in two main groups “up-hill” and “down-hill” [4]. This classification is related to thermodynamic principles involved in the reaction. In the case of photocatalytic hydrogen production the reaction is classified as “up-hill” reaction since that generates a large positive change of Gibbs energy i.e. photon energy is converted into chemical energy using the semiconductor material [4, 21, 22].

The first report of the use of a photocatalytic process to obtain hydrogen was published in 1972 by Fujishima and Honda [1]. This work received some attention from the scientific world, leading to a numerous related studies after its publication. Many of these works were developed to demonstrate the efficiency of irradiating TiO<sub>2</sub> within the UV -Vis. spectral range.

Although various chalcogenides (oxides and sulfides) have been used as semiconductors in photocatalytic reactions including ZnO, CeO<sub>2</sub>, ZrO<sub>2</sub>, SnO<sub>2</sub>, SbrO<sub>4</sub>, CdS, ZnS, etc., TiO<sub>2</sub> is considered the benchmark photocatalyst. The high efficiency and photostability in combination with the low cost and harmless properties often presents best photocatalytic performance when compared to the materials mentioned before [6, 22] .

This metal oxide can be found in three mineral forms: anatase, rutile and brookite. Rutile and anatase have been used and studied in the photocatalytic hydrogen production and photocatalytic water and air treatment. In spite of many works around the rutile form have

been developed, the anatase is the largely accepted as the most active polymorph in catalytic applications, especially for the decomposition of water molecule in hydrogen and oxygen [23, 24].

Once that bare  $\text{TiO}_2$  is inactive for hydrogen production the impregnation of some metals is necessary. They are named co-catalysts [22]. The activity of catalyst not only depends from the microstructure and physical properties but the type of metal loaded and supports incorporated. Some works demonstrate that the photocatalytic activity could be increased by modifications of the semiconductor's surface with metal nanoparticles [25], which act as co-catalysts. Usually the co-catalyst is a noble metal such as Pt, Ru (Ruthenium), Pd, Ag, Rh (Rhodium), Au, etc [26, 27]. The amount of loaded metal is important since that usually higher amounts increase the efficiency. Although the quantity of metal loaded should be considered since that excess of metal loaded in the catalyst surface leads to aggregation of metal particles and then reduces the activity of catalyst [27]. An equilibrium should be found and some percentages of metal loading was reported and the most common is find catalysts with co-catalysts in the surface in an amount between 0.5% - 2% in order to get the best results [4, 10, 27, 28]. There are also studies on the use of a combination of two or more metals ( usually name bimetallic in case of being two metal loaded) for the hydrogen production [29]. Pt is the most used co-catalyst due the lowest overpotential and for usually shows the highest activity in hydrogen production [22].

This contributes for a higher efficiency in the hydrogen production, since metals can act as electron buffers, decreasing the undesired recombination phenomena and also increasing the lifetime of the charge separation state. Several reports shows that the use of Pt as co-catalyst produces higher amounts of hydrogen when compared to other type of metals [30].

Another technique for improving the photoefficiency of  $\text{TiO}_2$  consists in the introduction of carbon materials such as graphene oxide, carbon nitride and carbon nanotubes (CNTs), to form  $\text{TiO}_2$ -based hybrids. The use of CNT-containing  $\text{TiO}_2$  composites has been reported to result on a significant improvement in hydrogen production comparing with bare  $\text{TiO}_2$  [31]. The classification of  $\text{TiO}_2$  combined with carbon materials could be separated in three types depending of state of carbon [24]:

- $\text{TiO}_2$ -loaded carbons
- carbon-doped  $\text{TiO}_2$  (or carbon-modified  $\text{TiO}_2$ )
- carbon-coated  $\text{TiO}_2$

For  $\text{TiO}_2$ -loaded carbons, the semiconductor is disperse in the carbon phase and inhibits the agglomeration of  $\text{TiO}_2$  particle [32]; in carbon-doped  $\text{TiO}_2$ , carbon substitutes the oxygen or titanium atom of  $\text{TiO}_2$ ; in carbon-coated  $\text{TiO}_2$  the semiconductor is layered with carbon. With

the advance in science and with the development of new materials, CNTs have been replacing activated carbon in many fields of application [33]. Due to the high chemical stability of CNTs, functionalization assumes an important role since for anchoring metal nanoparticles or semiconductor phases [33].

The efficiency of such hybrid materials has shown to be dependent on the CNT content and on the irradiation wavelength [31, 34, 35]. It has been reported that using a TiO<sub>2</sub>-CNT catalyst with 1% Pt loading under visible light irradiation some activity in the hydrogen production is observed while no H<sub>2</sub> production was achieved using TiO<sub>2</sub>, using both phenol and triethanolamine (TEOA) as sacrificial reagents [34, 35]. This is an interesting fact since only 5% of the total solar irradiation reaching Earth's surface can be adsorbed by TiO<sub>2</sub> (the UV part). Using the composite, the range of spectra of solar light that could be adsorbed by the catalyst is larger, which leads to an increase in the efficiency of the catalyst.

## 2.3 Biomass

Biomass compounds are carbon-based and are composed of a mixture of organic molecules containing hydrogen, usually including atoms of oxygen, often nitrogen and also small quantities of other atoms, including alkali, alkaline earth and heavy metals.

Various techniques are used to obtain hydrogen and other products from biomass such as thermochemical (pyrolysis, liquefaction and gasification) and biological (biophotolysis, water-gas shift reaction and fermentation) processes [9, 36]. Some works reporting the photocatalytic production of hydrogen were carried out using biomass-derived components and derivatives such as saccharides, alcohols and organic acids [8, 37].

Alcohols normally show good efficiency as sacrificial reagents in photocatalytic hydrogen production [22, 38]. Methanol is commonly used as sacrificial reagent for the photocatalytic production of hydrogen [4, 10, 25, 39-41]. Methanol is a biomass-derived liquid fuel. It is a clear, colourless, volatile liquid with a weak odour, which is used as feedstock in industrial production of many synthetic organic compounds and is a constituent of a large number of commercially available solvents.

Another important class of biomass-derived compounds successfully used for H<sub>2</sub> production via photocatalytic reforming process are saccharides such as glucose, sucrose, lactose, cellobiose, maltose, starch and cellulose [4, 42]. The rates of hydrogen evolution are usually higher for lactose, cellobiose, maltose and lower for cellulose and starch [42].

The relative efficiency for producing H<sub>2</sub> from such compounds has been the focus on intense investigation, being attributed to diverse reasons including the complexity of the carbon skeleton [4], the stoichiometry (C:H:O ratio) of the molecule [42] and/or the presence and

amount of  $\alpha$ -hydrogens atoms in the molecule structure, since in the case of tertiary alcohols for example, the inexistence of  $\alpha$ -hydrogens is pointed out as the main cause for the absence of hydrogen production when these compounds are used as biomass source [4, 37].

## 3 Materials and Methods

### 3.1 Catalysts synthesis

For the functionalization of the carbon nanotubes, 0.5 g of pristine CNT were immersed in 150 mL of 10 mol L<sup>-1</sup> nitric acid (HNO<sub>3</sub>) solution (prepared from 65 wt. % HNO<sub>3</sub>, Fluka). The suspension was heated to boiling temperature and kept under magnetic stirring for 3 h in a round bottom flask equipped with a condenser. After cooling, the suspension was washed several times with distilled water, until neutrality of the rinsing waters. The recovered powders were stored after being dried overnight at 110 °C.

CNT<sub>ox</sub>-TiO<sub>2</sub> composite was prepared using 0.1 g of functionalized CNT and 0.5 g of the TiO<sub>2</sub> powder, which were dispersed in 1 L of distilled water under ultrasonication. The mixture was heated up to 80 °C until complete evaporation of water. The composites were dried overnight at 110 °C to eliminate the remaining humidity before being stored.

For the synthesis of (CNT-TiO<sub>2</sub>)<sub>ox</sub>, the same experimental procedure described for the functionalization of CNT was used, both CNT and TiO<sub>2</sub> being added at the same time to the HNO<sub>3</sub> solution.

Metal loading was performed by incipient wetness impregnation, from aqueous solutions of the corresponding metal salts (PdCl<sub>2</sub>, HAuCl<sub>4</sub>·3H<sub>2</sub>O, (NH<sub>4</sub>)<sub>3</sub>IrCl<sub>6</sub>, H<sub>2</sub>PtCl<sub>6</sub>). The metal content was fixed at 1% (weight percent). After impregnation, the samples were dried at 100 °C for 24 h. The catalysts were heat treated under nitrogen flow for 1 h and reduced under hydrogen flow for 3 h at 200 °C or 400 °C.

### 3.2 Catalysts characterization

Observations of the morphology of the powder materials were performed using scanning electron microscopy (SEM) with a FEI Quanta 400FEG ESEM instrument. Elemental analysis of the prepared catalysts was performed by energy-dispersive X-ray spectroscopy (EDXS) using an EDAX Genesis X4M instrument. Transmission electron microscopy (TEM) was performed in a LEO 906E instrument operating at 120 kV, equipped with a 4 M pixel 28×28 mm CCD camera from TRS.

X-ray diffraction (XRD) analysis was carried out in a PANalytical X'Pert MPD equipped with a X'Celerator detector and secondary monochromator (Cu Ka  $\lambda$  = 0.154 nm, 50 kV, 40 mA; data recorded at a 0.0178 step size, 100 s/step). Rietveld refinement with PowderCell software

was used to identify the crystallographic phases present and to calculate the crystallite size from the XRD diffraction patterns.

The textural characterization of the materials was based on the corresponding N<sub>2</sub> adsorption-desorption isotherms at -196 °C, measured on a Quantachrome NOVA 4200e multi-station apparatus. All samples were first degassed in vacuum for 3 h at 120 °C before analysis. The BET specific area ( $S_{\text{BET}}$ ) was calculated from the nitrogen adsorption data in the relative pressure range 0.05-0.15.

Temperature programmed desorption (TPD) and temperature programmed reduction (TPR) analysis were carried out using an AMI-200 instrument (Altamira Instruments) equipped with a quadrupole mass spectrometer (Ametek, Mod. Dymaxion). For TPD analysis the sample (0.1 g) was placed in a U-shaped quartz tube and heated at 5 °C min<sup>-1</sup> in an electrical furnace under a constant flow of 25 cm<sup>3</sup> min<sup>-1</sup> (STP) of helium, used as carrier gas.

The TPR experiments a sample (150 mg) was heated at 5 °C min<sup>-1</sup> up to 600 °C under a flow of 5% (v/v) H<sub>2</sub> diluted with He (total flowrate of 30 Ncm<sup>3</sup>min<sup>-1</sup>). The H<sub>2</sub> consumption was followed by the thermal conductivity detector (TCD) and by a mass spectrometer (Dymaxion 200 amu, Ametek).

UV-Vis diffuse reflectance spectra (220-800 nm) of the powder samples were recorded on a JASCO V-560 UV-Vis spectrophotometer, with a double monochromator, double beam optical system. The spectrophotometer was equipped with an integrating sphere attachment (JASCO ISV-469). The reflectance spectra were converted by the instrument software (JASCO) to equivalent absorption Kubelka-Munk units. Attenuated total reflectance (ATR) analysis were performed using a MIRacle Single Reflection ATR (ZnSe crystal plate) accessory (PIKE Technologies, USA) in a Nicolet 510P FTIR spectrometer, with a KBr beam splitter for mid-IR range and a DTGS with KBr windows equipped with a special beam collector (COLLECTOR from Spectra Tech), fixed on a plate for consistent experimental conditions. The interferograms were converted by the instrument software (OMINC) to equivalent absorption units in the Kubelka-Munk scale.

### 3.3 Photocatalytic reactions

The photocatalytic runs were carried out in a cylindrical glass immersion photo-reactor equipped with a Heraeus TQ 150 medium pressure mercury vapour lamp ( $\lambda_{\text{exc}} = 254, 313, 365, 436$  and  $546$  nm) located axially in the reactor and held in a quartz immersion tube. A DURAN® glass cooling jacket was used for irradiation in the near-UV to visible light range ( $\lambda_{\text{exc}} \geq 365$  nm). During the photocatalytic experiments, the temperature was maintained at around

25 °C. The reactor was charged with 220 mL of the aqueous solution of methanol (10% vol.) or saccharide (0.02 M) and 220 mg (catalyst load of 1 g L<sup>-1</sup>). The suspension was first degassed by a nitrogen flow for 20 min and then the light was turned on. During measurements, the N<sub>2</sub> flow was maintained at 10 cm<sup>3</sup> min<sup>-1</sup>. Hydrogen was detected on line by using an Inficon Micro GC 3000 gas chromatograph equipped with a molsieve column and a micro-TCD detector, using argon as carrier gas. In Figure 2 is represented a schema from the installation where the reactions were carried on.

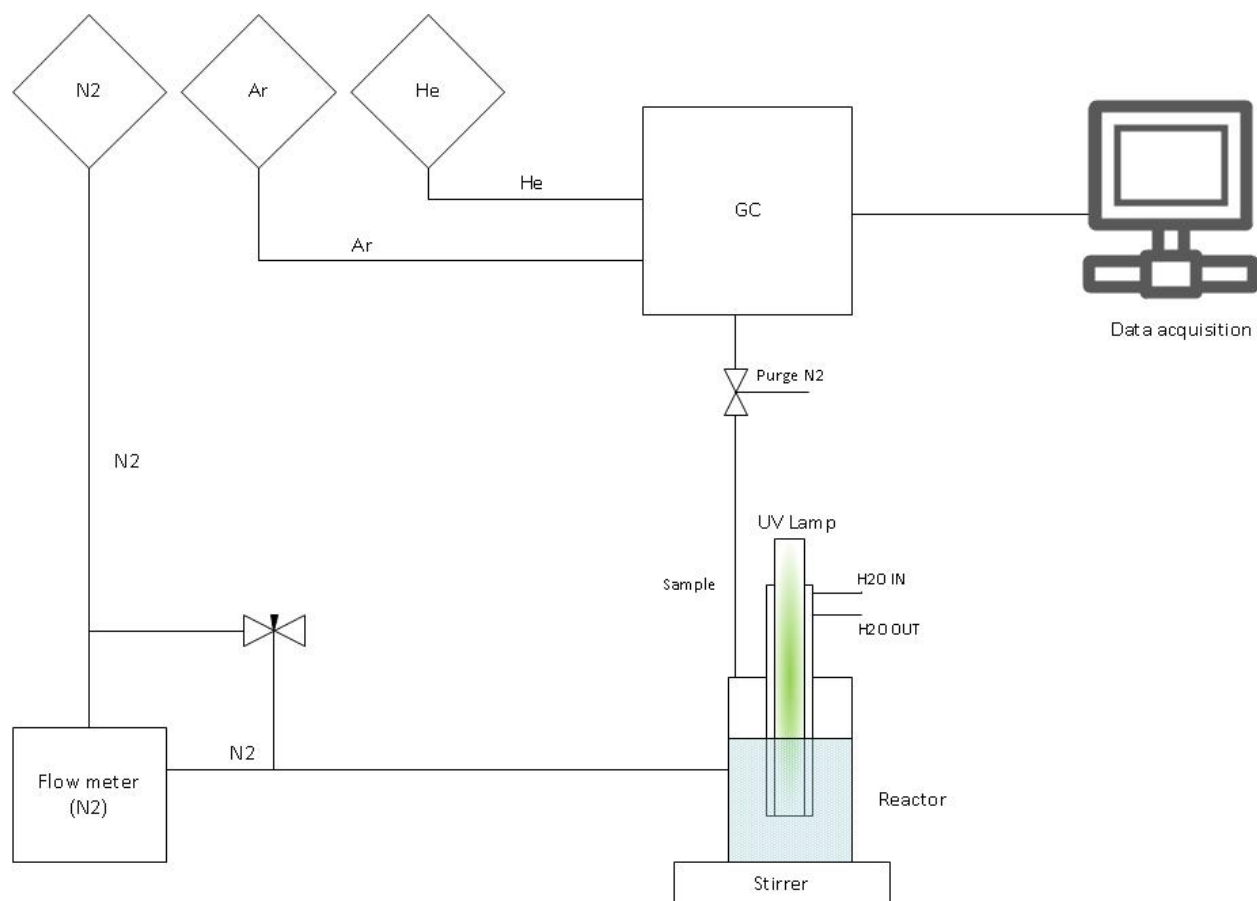


Figure 2. Schematic representation of reaction setup.

## 4 Results and discussion

### 4.1 Catalysts characterization

The catalysts were analysed with various techniques where some crystalline, morphological, textural and optical characteristics from material were evaluated.

X-ray diffraction (XRD) patterns of the catalysts were analysed and they are presented on Figure 3.

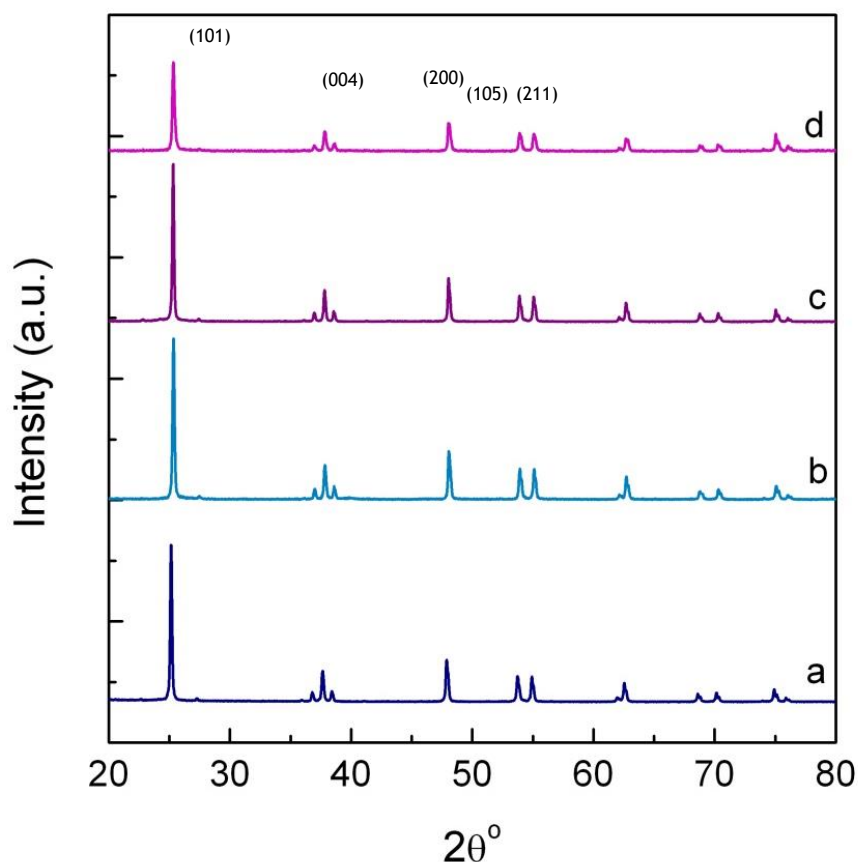


Figure 3. XRD patterns of  $\text{TiO}_2$  (a),  $1\% \text{Pt}/\text{TiO}_2$  (b),  $(\text{CNT-TiO}_2)_{\text{ox}}$  (c) and  $1\% \text{Pt}/(\text{CNT-TiO}_2)_{\text{ox}}$  (d).

On the patterns presented here, only the anatase phase can be identified, so the thermal treatment for metal loading didn't change the crystalline form of the original material. It is visible a similarity in all the peaks for the different materials. The mainly difference is in the intensity of the peaks obtained for  $1\% \text{Pt}/(\text{CNT-TiO}_2)_{\text{ox}}$ . Nevertheless, the relative intensity of those peaks remains the same as for the other materials.

The dimensions for anatase crystallites ( $x_{\text{anatase}}$ ), determined by Rietveld refinement with PowderCell software, were estimated to be in the order of 70 nm.

In table 1 it is shown some properties of  $\text{TiO}_2$ , CNT and  $(\text{CNT-TiO}_2)_{\text{ox}}$  materials. The  $\text{N}_2$  adsorption-desorption isotherms can be classified as type II (Appendix A), according to IUPAC classification, which occur in non-porous or macroporous materials [43, 44]. In the presence case it must be due to the adsorption of  $\text{N}_2$  on the sidewalls of the materials. The Brunauer-Emmett-Teller (BET) surface area ( $S_{\text{BET}}$ ) for each catalyst used is presented on Table 1. As expected, CNT has the highest BET area while the composite presents a surface area comprised between those of neat CNT and  $\text{TiO}_2$ . This value for the composite is justified for the fact that CNT works as dispersion media for  $\text{TiO}_2$  and then avoid the agglomeration of  $\text{TiO}_2$  particles. The carbon load was determined by TG analysis ( $C_{\text{TG}}$ ). For CNTs this value is 100% as expected since that the structure is constituted by carbon. For the hybrid material the value is in agreement with the theoretical one. The weight ratio of CNT: $\text{TiO}_2$  used in for producing the composite was of 20 parts of CNTs per 100 parts of  $\text{TiO}_2$ , which corresponds to a theoretical carbon content of 16.7%.

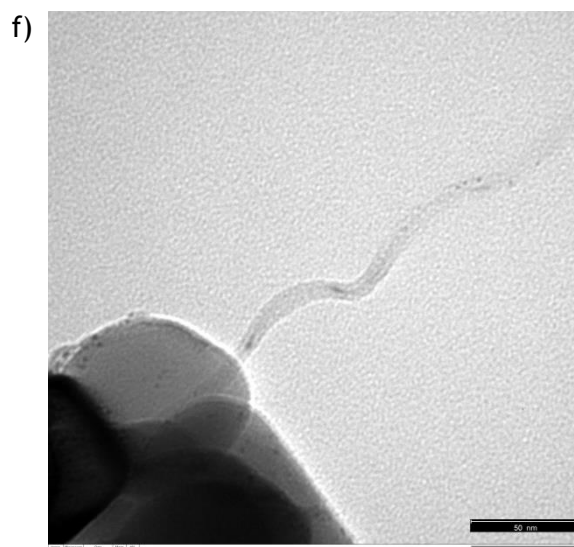
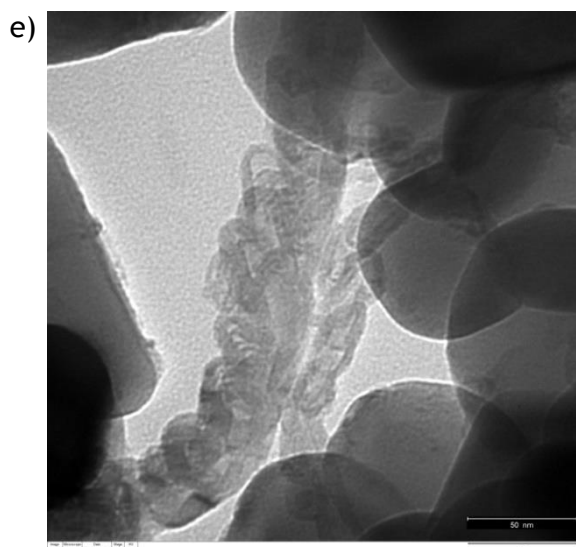
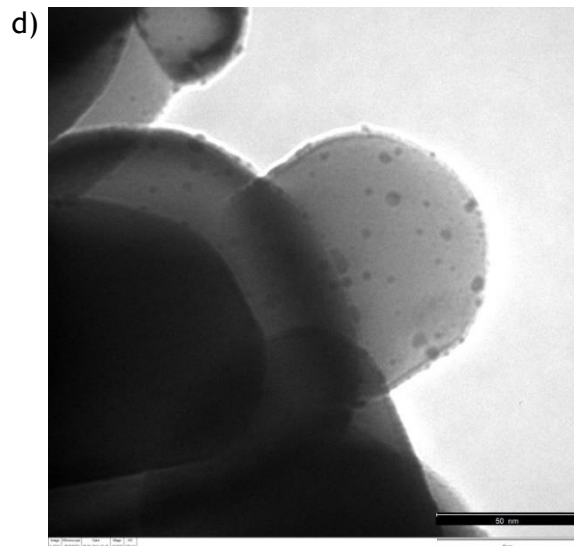
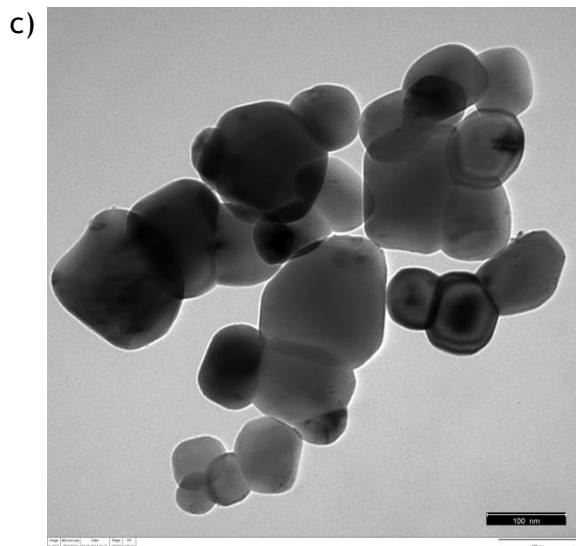
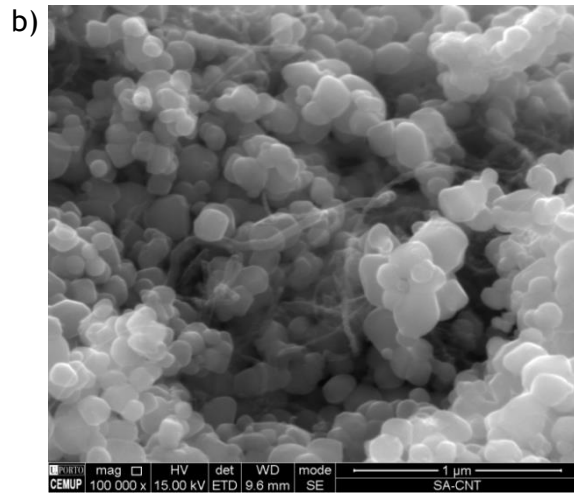
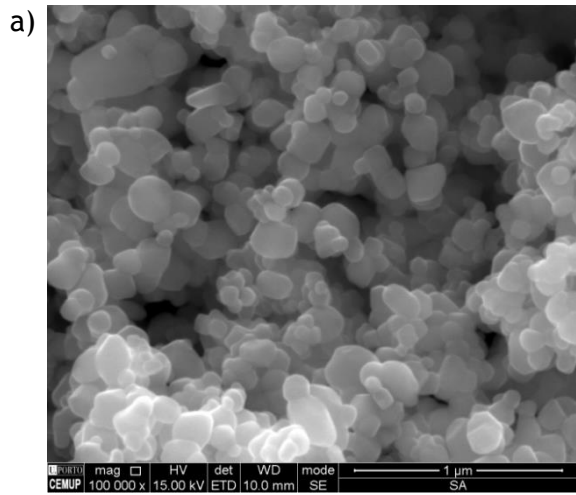
*Table 1. BET surface area ( $S_{\text{BET}}$ ), and anatase ( $x_{\text{anatase}}$ ) and carbon ( $C_{\text{TG}}$ ) contents of the used materials.*

Material	$S_{\text{BET}}$ ( $\text{m}^2/\text{g}$ )	$x_{\text{anatase}}$ (%)	$C_{\text{TG}}$ (%)
CNT	374	n.a. <sup>[a]</sup>	100
$\text{TiO}_2$	11	100	n.a. <sup>[a]</sup>
$(\text{CNT-TiO}_2)_{\text{ox}}$	61	100	16.8
[a] Not applicable			

In Figure 4 are presented SEM images of the synthesized material, where it is possible to see the particles of  $\text{TiO}_2$  in (a) and the nanotubes combined within  $\text{TiO}_2$  in (b). In the TEM images the Pt particles are visible as little black dots on the surface of  $\text{TiO}_2$  (d) and CNTs surface too in (f). In (e) it can be observed the contact between  $\text{TiO}_2$  and CNTs. In the EDX spectrum is possible to identify the presence of Pt, Ti and O elements (g).

The carbon peak in the EDX spectrum occurs due to the presence of CNT, but a contribution from the sample support is also expected.

The presence of Cl can be attributed to some metal precursor used for impregnate Pt in the catalyst, which was not totally removed during the thermal treatment.



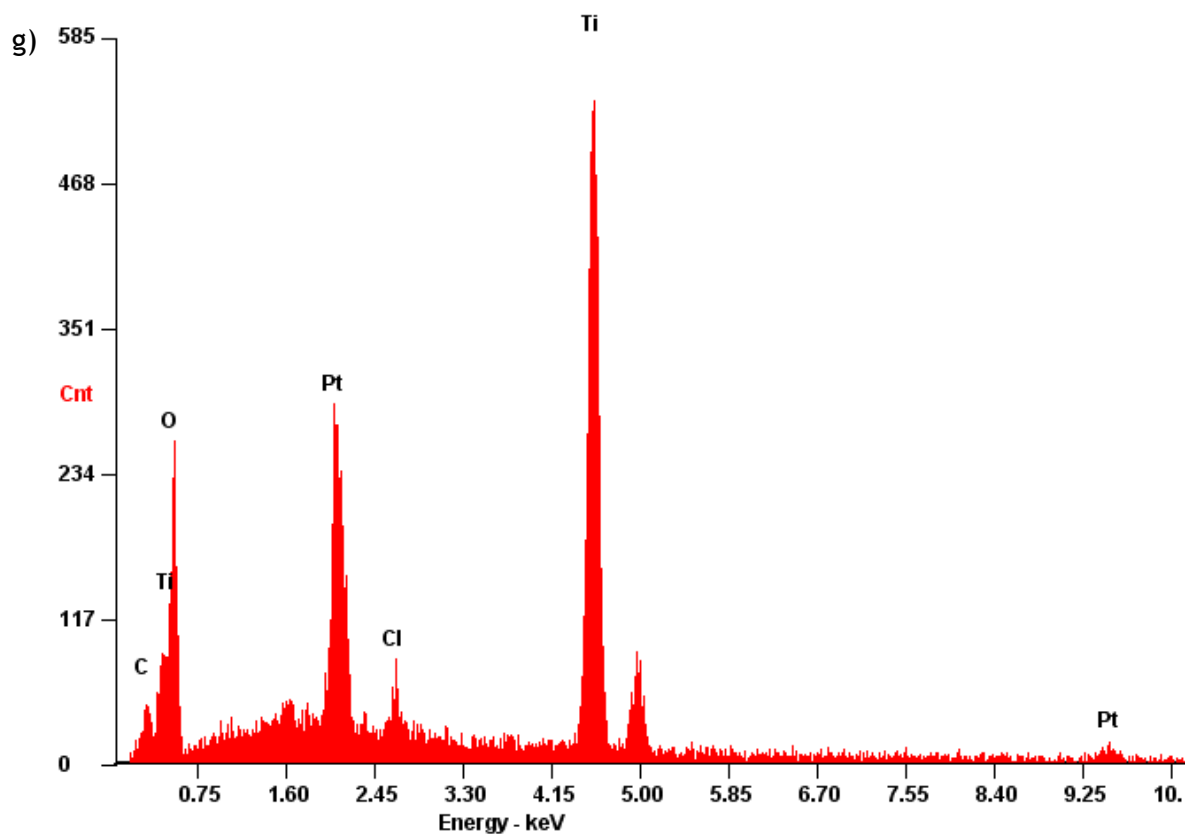


Figure 4. SEM images of  $\text{TiO}_2$  (a) and composite  $(\text{CNT-TiO}_2)\text{ox}$  (b), and TEM images of 1% Pt/ $\text{TiO}_2$  (c) and (d), and 1% Pt/ $(\text{CNT-TiO}_2)\text{ox}$  (e) and (f). EDX spectrum obtained from analysis of the 1% Pt/ $(\text{CNT-TiO}_2)\text{ox}$  catalyst in zone Z1 (see Appendix A)(g)

Attenuated Total Reflectance (ATR) is a simple technique used with infrared spectroscopy that allows the direct analysis of a solid or liquid without a previous preparation of the sample. In Figure 5 are represented the analysis submitted to  $\text{TiO}_2$  and to the hybrid materials with different treatments:  $\text{CNTox-TiO}_2$  and  $(\text{CNT-TiO}_2)\text{ox}$ .

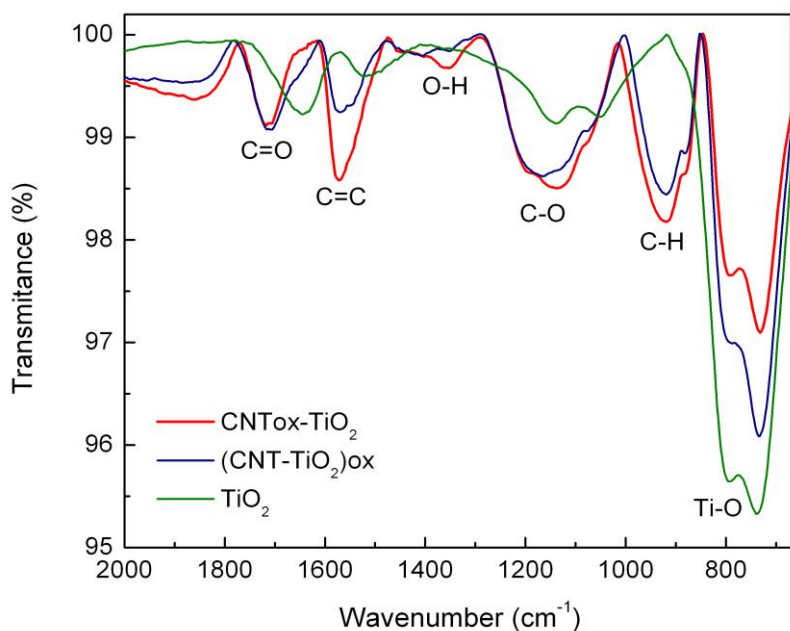


Figure 5. Attenuated Total Reflectance (ATR) spectra of  $\text{TiO}_2$ ,  $\text{CNTox-TiO}_2$  and  $(\text{CNT-TiO}_2)\text{ox}$ .

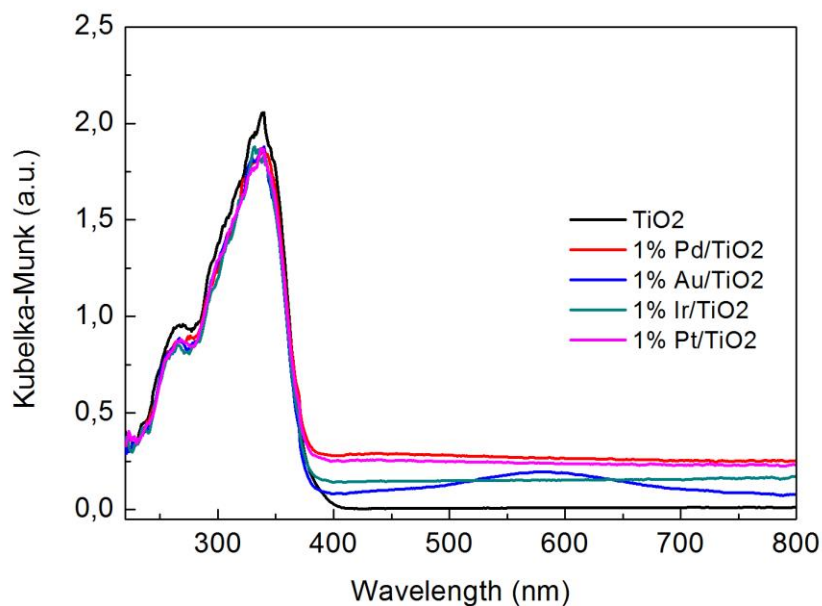
Typical bands of alcohols, carboxylic acid, ethers, esters, carboxylic anhydrides, phenols, carbonyl, quinones and lactones can be observed for both  $\text{CNT-TiO}_2$  composites. These bands are from the functionalization of CNTs where some groups were created on the surface.

In the case of  $(\text{CNT-TiO}_2)\text{ox}$  a decrease in the intensity of the bands corresponding to C=C (alkene), O-H, C-H and C-O indicate that  $\text{TiO}_2$  may be anchored to carboxylic acid and phenol groups so the number of these groups is reduced. These results indicate that a better interphase interaction is promoted by the *in situ* functionalization of CNT during the composite preparation.

For all of these studied materials, Ti-O band appears and is more accentuated in  $\text{TiO}_2$  than in other materials. This means the existence of more groups of Ti-O in  $\text{TiO}_2$  than in other materials. The appearance of this band in all materials proves that  $\text{TiO}_2$  exists in all of them.

One of the most important type of analysis of photocatalysts is the methods related to the optical absorption spectrum. The Diffused Reflectance UV-Visible (DR UV-Vis.) spectra of the catalysts used with different loaded metals, expressed in Kubelka-Munk equivalent absorption units, are presented in the Figure 6.

a)



b)

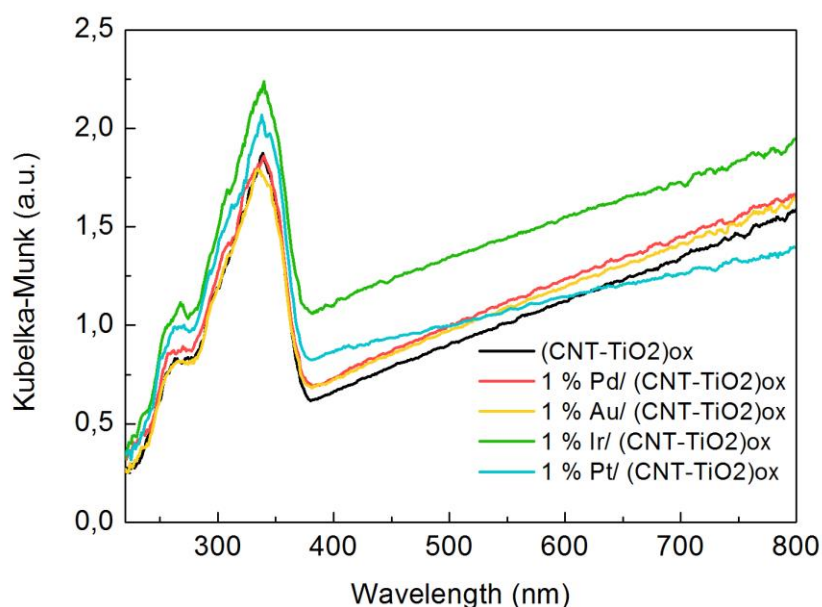


Figure 6. Diffused reflectance UV-Vis. (DR-UV Vis.) spectra of different catalysts:  $\text{TiO}_2$  (a) and  $(\text{CNT-TiO}_2)_{\text{ox}}$  (b) with different metals loaded.

As expected,  $\text{TiO}_2$  has no absorption above its fundamental absorption sharp edge rising at 400 nm. There are some similarities between the  $\text{TiO}_2$  and  $(\text{CNT-TiO}_2)_{\text{ox}}$  catalysts, with the main peak appearing at wavelengths lower than 400 nm, attributed to anatase absorption. In the case of metal-loaded  $\text{TiO}_2$ , higher adsorption in the visible range was observed for Pt and Pd containing materials. In case of  $\text{Au/TiO}_2$  (Figure 6.a) it is visible a peak centred between

550 and 600 nm that indicates the presence of the gold plasmonic absorption. Gold itself has the capacity to be photoexcited by means of a surface plasmon resonance effect [45].

The introduction of CNTs in the  $\text{TiO}_2$  leads to an increase in the absorption mostly in the visible spectral range, as observed in Figure 6.b). This phenomenon is due the existence of CNT in the catalyst matrix. This presence leads to a small increase in the absorption edge, which indicates a decrease in the band gap energy for these materials.

With this analysis we are able to see that the light source used in this work is appropriated to carry the reaction since all materials absorbs in the range of lamp emission.

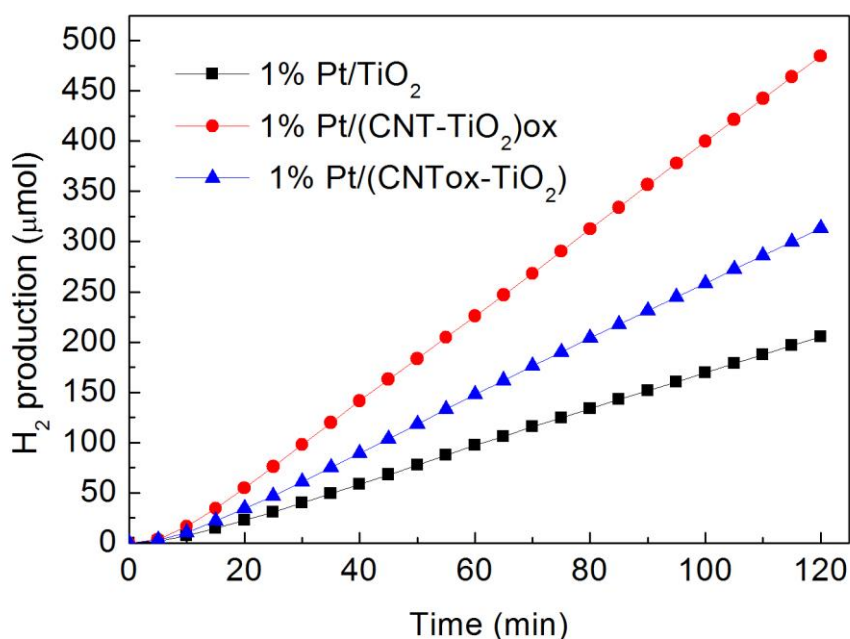
## 4.2 Photocatalytic results

### 4.2.1 Photocatalytic hydrogen generation from methanol

#### 4.2.1.1 Effect of the type of CNT- $\text{TiO}_2$ composite

Preliminary tests on  $\text{H}_2$  production from methanol using 1% Pt-loaded  $\text{TiO}_2$  produced at 200 °C revealed that the highest amount of hydrogen was obtained with a catalyst load of 1 g L<sup>-1</sup>. Therefore this value was fixed for all the catalysts used. The comparison of results was performed with 1% Pt loaded  $\text{TiO}_2$  and  $\text{TiO}_2$  combined with CNT by two methods: simple mixing both phases, CNTox- $\text{TiO}_2$ , and by *in situ* functionalization, (CNT- $\text{TiO}_2$ )ox (Figure 7).

a)



b)

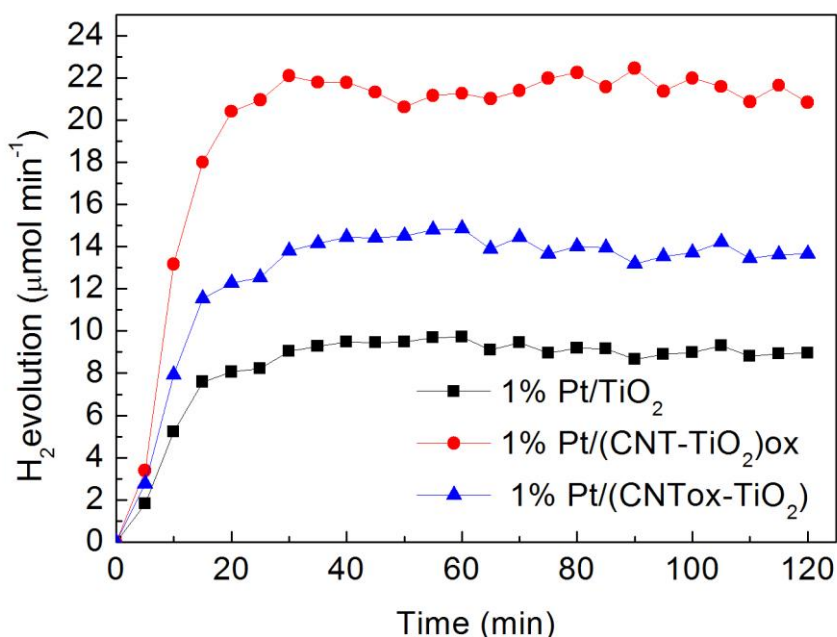


Figure 7. Hydrogen production (cumulative) (a) and profiles (b) using different catalysts with loaded with 1% Pt in a 10% vol. methanol aqueous solution.

From Figure 7 it can be seen that all the tested catalysts promote hydrogen generation but in different amounts. In Figure 7.a) it is visible that the hybrid materials *i.e.* the materials that contains TiO<sub>2</sub> and CNT, produces higher amounts of hydrogen than only TiO<sub>2</sub>. These results may be related to CNTs electronic properties, which facilitates electron mobility in the resulting composite material. In the group of hybrid materials it was verified that the material that was oxidized *in situ* - (CNT-TiO<sub>2</sub>)<sub>ox</sub> - shows better results than the one in which CNTs was functionalized and then added to TiO<sub>2</sub> (CNT<sub>ox</sub>-TiO<sub>2</sub>). This behaviour can be attributed to the different synthesis procedures used for obtaining both materials. When CNTs are functionalized together with TiO<sub>2</sub>, the groups created at the surface of CNTs links at same time to the TiO<sub>2</sub> surface groups, resulting in a stronger interaction between both phases and promoting a higher homogeneity of the resulting material when compared to CNT<sub>ox</sub>-TiO<sub>2</sub>. For CNT<sub>ox</sub>-TiO<sub>2</sub>, CNTs are functionalized and then the TiO<sub>2</sub> is added, so the interactions between the surface of both materials are weaker and the material is more heterogeneous. These results are in agreement with the ATR characterization, where a decrease of the intensity of the surface bands of CNT is observed for (CNT-TiO<sub>2</sub>)<sub>ox</sub> due to the stronger interphase interaction.

#### 4.2.1.2 Effect of the nature of the co-catalyst

The co-catalyst is an important element in photocatalytic hydrogen production reactions. The role of the metal co-catalyst is to retain and transfer the electrons. Several properties of metal-loaded semiconductors may change depending on the calcination and reducing temperatures [28].

Temperature Programmed Reduction (TPR) analysis of TiO<sub>2</sub> impregnated with each metal precursor was performed in order to determine the reduction temperature of each metal (Figure 8). The peaks correspond to the H<sub>2</sub> consumption during the thermal treatment.

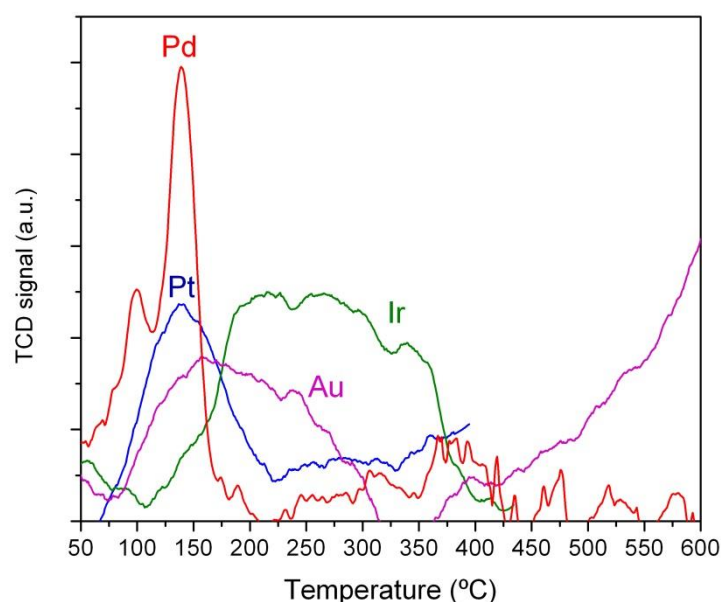
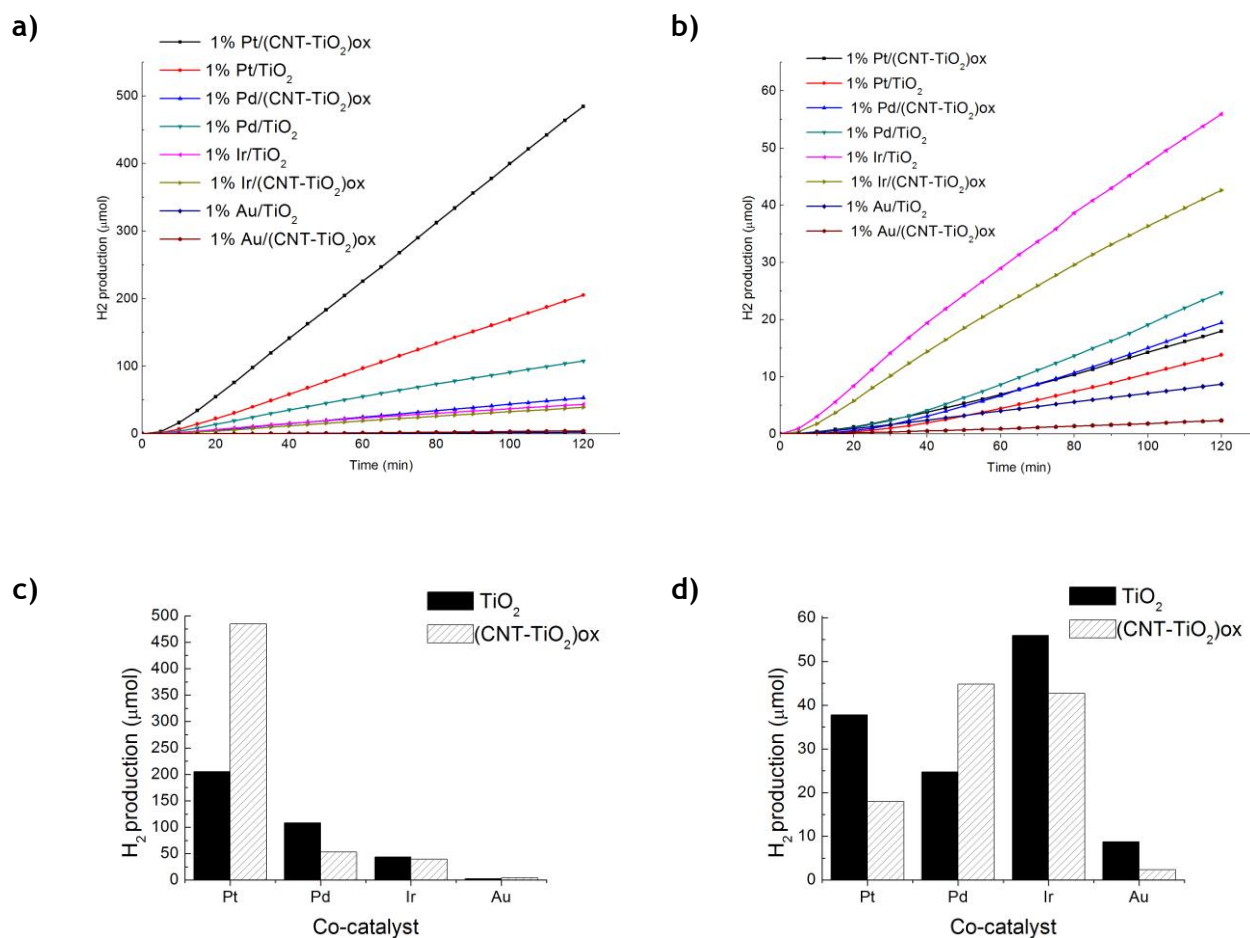


Figure 8. TPR for co-catalysts: Pt(blue), Pd (red), Au (violet) and Ir (green).

In Figure 8 it is clear that Pd-loaded TiO<sub>2</sub> presents the most intense reduction peak followed by Pt, both at around 100-200 °C. The Ir reduction peak is large and has a wide range of temperatures, between 100 and 400 °C. Au-loaded TiO<sub>2</sub> shows a broad peak between 100 and 300 °C. Having these results into consideration, each metal was impregnated in TiO<sub>2</sub> and (CNT-TiO<sub>2</sub>)<sub>ox</sub> and calcined/reduced at two different temperatures: 200 °C and 400°C. Thermal treatments at higher temperatures were not tested to avoid metal particle sinterization and TiO<sub>2</sub> crystal phase transition from anatase to rutile.

The effect of metal reduction temperature on the efficiency of H<sub>2</sub> generation from 10% wt. methanol solutions was studied using the different metal-loaded catalysts (Figure 9).



**Figure 9.** Cumulative production of hydrogen and total amount of hydrogen produced respectively during 120 minutes for catalysts treated at 200°C (a), (c) and at 400°C (b), (d) in 10 % Methanol solution.

For the materials reduced at 200°C, in general the hybrid (CNT-TiO<sub>2</sub>)<sub>ox</sub> catalysts show higher amounts of hydrogen produced when compared to the same metal loading but in TiO<sub>2</sub>.

The catalysts that lead to the highest amounts of hydrogen produced were 1% Pt/(CNT-TiO<sub>2</sub>)<sub>ox</sub> (485 μmol) and 1% Pt/TiO<sub>2</sub> (205 μmol), both reduced at 200°C (Figure 9.e) .

Pd-loaded materials also present a significant amount of hydrogen production for this treatment temperature as expected based on TPR analysis. Nevertheless, in this case, neat TiO<sub>2</sub> show best results than the corresponding composite material. In the case of Ir-loaded catalysts, no significant difference was observed between the amount of H<sub>2</sub> generated from TiO<sub>2</sub> and from the composite material, with 44 and 39 μmol of H<sub>2</sub> generated at the end of 120 min of irradiation, respectively. Finally, Au-loaded materials were the less efficient catalysts, with only 2.4 and 4.5 μmol of H<sub>2</sub> being obtained with the neat and composite material, respectively.

For the experiments using the Ir and Au materials calcined and reduced at 400 °C, it was observed an increase in H<sub>2</sub> generation when compared with those produced at 200 °C (Figure 9.f). These results are in line with the TPR results (Figure 8), since for these metals, complete reduction is only achieved at temperatures higher than 200 °C. Nevertheless, for the experiments carried out with the materials obtained at 400 °C, more hydrogen was produced with TiO<sub>2</sub>-based catalysts than with (CNT-TiO<sub>2</sub>)<sub>ox</sub>, except in the case of Pd-loaded catalysts. This probably occurs because of the sinterization phenomena that may happen when the metal-loaded composite materials are submitted to high temperatures.

From here it can be defined that the best co-catalyst is Pt with better results in TiO<sub>2</sub> and (CNT-TiO<sub>2</sub>)<sub>ox</sub> being obtained for the catalysts reduced at 200 °C. Therefore, 1%Pt/TiO<sub>2</sub> and 1%/(CNT-TiO<sub>2</sub>)<sub>ox</sub> reduced at 200°C were used for further studies on hydrogen generation from the photocatalytic reforming of saccharides.

#### 4.2.2 Photocatalytic hydrogen generation from saccharides

After testing the production of hydrogen with different catalysts and co-catalysts, another important variable to be studied in photocatalytic reforming reactions is the nature of the sacrificial reagent. The selected approach was to use different saccharides, which are compounds that can be considered as wastes or by-products of several industrial activities, including some with similar molecular formula but different structure: fructose, glucose, arabinose and cellobiose. The respective molecular structures are represented in Figure 10.

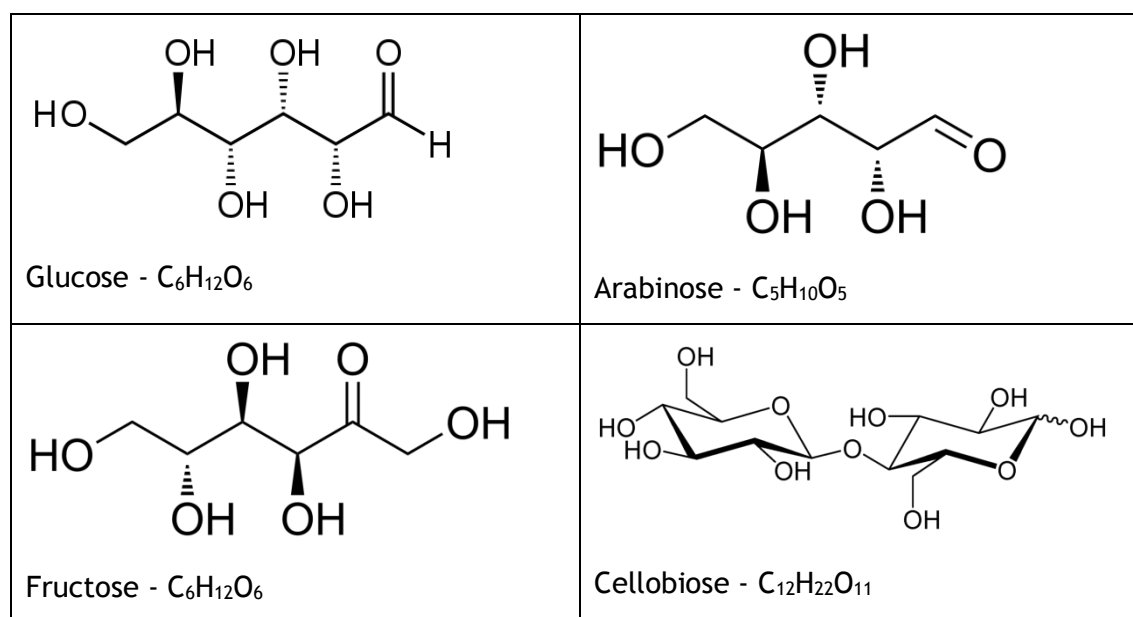
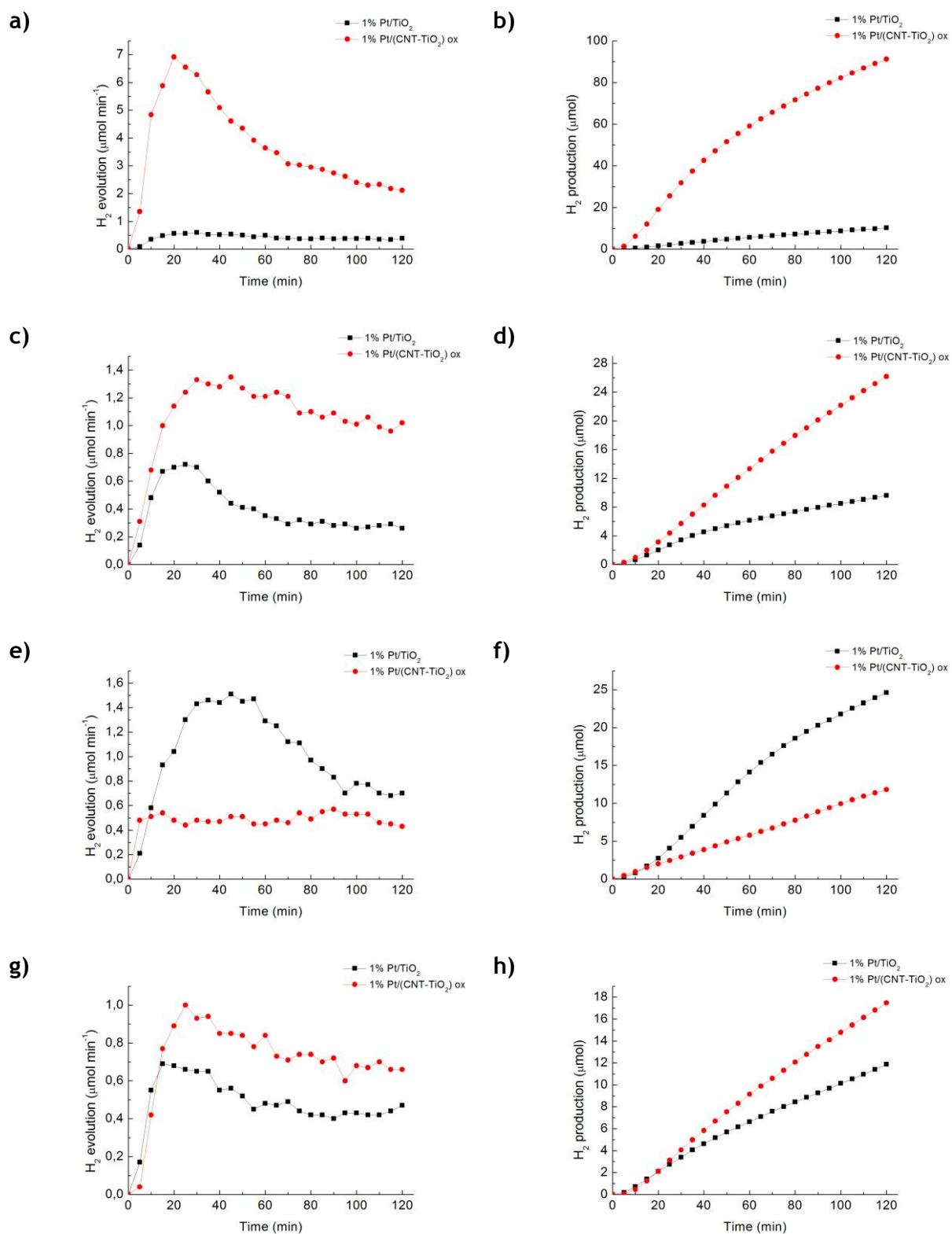


Figure 10. Saccharides molecular structure and respective molecular formula

The hydrogen evolution from 0.02 M aqueous solution of the different saccharides was followed for the reactions using Pt/TiO<sub>2</sub> and Pt/(CNT-TiO<sub>2</sub>)<sub>ox</sub> as catalyst. The H<sub>2</sub> generation profiles, cumulative H<sub>2</sub> production and total amount of H<sub>2</sub> produced at the end of 2h of irradiation are presented in Figure 11.



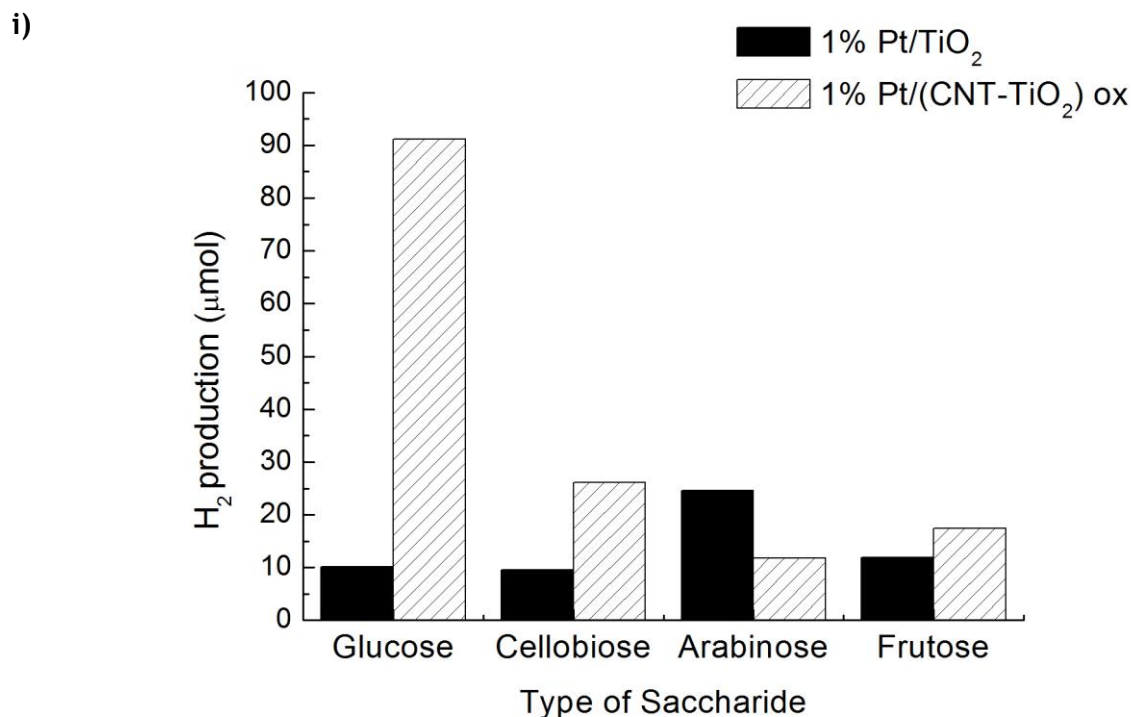
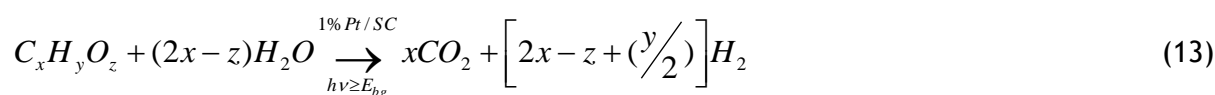


Figure 11. Evolution and production respectively of Hydrogen with glucose (a),(b); cellobiose (c),(d); arabinose (e),(f) and fructose (g),(h). Total amount of hydrogen produced with 1%Pt/TiO<sub>2</sub> and 1%Pt/(CNT-TiO<sub>2</sub>)ox for different saccharides solution (i).

It was observed that the use of the Pt-loaded (CNT-TiO<sub>2</sub>)ox catalyst resulted in higher amounts of H<sub>2</sub> generated when compared to Pt/TiO<sub>2</sub>, except for arabinose (Figure 11.i).

The relative efficiency of H<sub>2</sub> production from biomass sources can be related with different factors such as the C:H:O molar ratio in the molecular structure, the structural complexity of each compound and to the existence of α-hydrogens in its molecular structure, or most probably by a combination of them [4].

The theoretical amount of H<sub>2</sub> that can be generated from biomass-derived compounds can be described by the following equation [8]:



Applying this equation we should obtain (per mol of biomass):

- Glucose: 6 mols of H<sub>2</sub>
- Arabinose: 5 mols of H<sub>2</sub>
- Fructose: 6 mols of H<sub>2</sub>
- Cellobiose: 11 mols of H<sub>2</sub>

These could be valid for the production with 1% Pt/(CNT-TiO<sub>2</sub>)<sub>ox</sub> but not explain why with glucose the total amount of hydrogen produced is higher than with cellobiose.

In the case of the reactions using 1% Pt/TiO<sub>2</sub>, similar amounts of H<sub>2</sub> were obtained using fructose and glucose, which is in agreement with the above equation.

Other reason to different yields of hydrogen is the position of hydrogens in the molecular structure.  $\alpha$ -Hydrogens are hydrogens linked to the  $\alpha$ -carbon that it is the carbon positioned immediately to the functional group. Again this only explains the difference between glucose and fructose that have the same molecular formula and it is consistent with the results of hydrogen production with 1% Pt/TiO<sub>2</sub>.

Another explanation for the different results between saccharides is related with the complexity of carbon skeleton. Since that cellobiose is the saccharide that presents the most complex structure is expected that with this saccharide the amounts of H<sub>2</sub> generated were lower. Once again this is valid for 1%Pt/TiO<sub>2</sub> production.

It can be concluded that the different results of hydrogen production are a combination of various variables presented here. In fact, they could not be justified with only one independent theory but most probably by the combination of several factors which must be further investigated in future work. In spite of the different amount values of hydrogen produced, it is clear that the biomass, in this specific case, saccharides can be used in the hydrogen production as sacrificial reagent. This is a very significant result since it was demonstrated that aqueous solutions containing saccharides could be efficiently used for H<sub>2</sub> production. Ultimately, the vaporization of real waste streams (wastewaters, byproduct industrial streams) can be achieved by using the developed photocatalytic systems.

## 5 Conclusions

The photocatalytic hydrogen production from biomass was studied. Hydrogen was efficiently produced using metal-loaded CNT-TiO<sub>2</sub> catalysts. Some general conclusions could be inferred from the present work such as:

- Hybrid CNT-TiO<sub>2</sub> materials are generally more efficient than bare TiO<sub>2</sub>. The methods related to the functionalization of CNT and addition of TiO<sub>2</sub> has influence in the relative efficiency of the resulting catalysts.
- The type of co-catalyst has an important influence in the efficiency of H<sub>2</sub> production. The best results were obtained with the Pt-loaded materials.
- The yield of hydrogen is strongly related to the type of biomass solution used, the best results being obtained with glucose.
- Many variables contribute to the differences of H<sub>2</sub> generation efficiency observed for the different saccharides such as stoichiometry, carbon skeleton and the presence of  $\alpha$ -Hydrogens .

### 5.1 Accomplished Objectives

The main objective of this work was the photocatalytic production of hydrogen from biomass. The study of catalyst, co-catalyst and sacrificial reagent were some variables in study to determine which gives higher efficiencies in the production of the molecule.

With basis on the conclusions stated before it is fair to say that the objectives of the present work were successfully achieved.

### 5.2 Limitations and future work

The development of a system of hydrogen production from biomass is presented in this work. Despite the well-succeeded results, this project is far of being concluded and suggestions for future work is presented below, separated by different approaches.

#### Preparation of CNT/TiO<sub>2</sub> composites

In the present work the semiconductor metaloxide used was always the same: TiO<sub>2</sub> provided by Sigma-Aldrich. Other metal oxides and sulphides could be tested as well as other types of TiO<sub>2</sub>.

The metal loading is another parameter that could be further studied. The optimization of the metal percentage to obtain best results would be desired. Another interesting approach

would be the combination of two or more metals to know how the yield of hydrogen production is affected.

The type of metal-loading method should also be studied, since it is known that it greatly affect the properties of the resulting catalysts and ultimately the efficiency of hydrogen production.

### **Biomass Reforming**

The type of biomass is another condition that could be exhaustively studied since that exists various types of biomass-derived streams that comes from various type of industries as waste.

## **5.3 Final Appreciation**

The work developed in a laboratory environment allowed a first-time dealing with real problems and obstacles. The multidisciplinary, cultural and language team gave me some knowledge that only it is possible get with this type of communication. This work not only gave me a strong background in the fields of catalysis synthesis and photocatalytic processes but also some personal skills in communication and team work, which will be valuable for my personal and professional development.

## 6 References

1. Fujishima, A. and K. Honda, *Electrochemical Photolysis of Water at a Semiconductor Electrode*. *Nature*, 1972. **238**(5358): p. 37-38.
2. Veziroğlu, T.N. and S. Şahin, *21st Century's energy: Hydrogen energy system*. *Energy Conversion and Management*, 2008. **49**(7): p. 1820-1831.
3. Al-Mazroai, L.S., et al., *The photocatalytic reforming of methanol*. *Catalysis Today*, 2007. **122**(1-2): p. 46-50.
4. Cargnello, M., et al., *Photocatalytic H<sub>2</sub> and Added-Value By-Products - The Role of Metal Oxide Systems in Their Synthesis from Oxygenates*. *European Journal of Inorganic Chemistry*, 2011. **2011**(28): p. 4309-4323.
5. Faria, J., *The Heterogeneous Photocatalytic Process*, in *Catalysis from theory to application*. 2008, I. d. U. d. Coimbra, Editor: Coimbra. p. 477-494.
6. Herrmann, J.M., *Heterogeneous photocatalysis: State of the art and present applications*. *Topics in Catalysis*, 2005. **34**: p. 49-65.
7. Hashimoto, K., H. Irie, and A. Fujishima, *A Historical Overview and Future Prospects*. *AAPPS Bulletin*, 2007. **17**: p. 12-28.
8. Patsoura, a., D. Kondarides, and X. Verykios, *Photocatalytic degradation of organic pollutants with simultaneous production of hydrogen*. *Catalysis Today*, 2007. **124**: p. 94-102.
9. Ni, M., et al., *An overview of hydrogen production from biomass*. *Fuel Processing Technology*, 2006. **87**: p. 461-472.
10. Oros-Ruiz, S., et al., *Photocatalytic hydrogen production by water/methanol decomposition using Au/TiO<sub>2</sub> prepared by deposition-precipitation with urea*. *J Hazard Mater*, 2013. **263 Pt 1**: p. 2-10.
11. Slamet, et al., *Photocatalytic hydrogen production from glycerol-water mixture over Pt-N-TiO<sub>2</sub> nanotube photocatalyst*. *International Journal of Energy Research*, 2013. **37**(11): p. 1372-1381.
12. Iijima, S., *Helical microtubules of graphitic carbon*. *Nature*, 1991. **354**(6348): p. 56-58.
13. Paradise, M. and T. Goswami, *Carbon nanotubes - Production and industrial applications*. *Materials & Design*, 2007. **28**(5): p. 1477-1489.
14. Cargnello, M. and B.T. Diroll, *Tailoring photocatalytic nanostructures for sustainable hydrogen production*. *Nanoscale*, 2013. **6**: p. 97-105.
15. Ohtani, B., *Preparing Articles on Photocatalysis—Beyond the Illusions, Misconceptions, and Speculation*. *Chemistry Letters*, 2008. **37**(3): p. 216-229.
16. Chaubey, R., et al., *A review on development of industrial processes and emerging techniques for production of hydrogen from renewable and sustainable sources*. *Renewable and Sustainable Energy Reviews*, 2013. **23**: p. 443-462.
17. Holladay, J.D., et al., *An overview of hydrogen production technologies*. *Catalysis Today*, 2009. **139**(4): p. 244-260.
18. Haryanto, A., et al., *Current Status of Hydrogen Production Techniques by Steam Reforming of Ethanol: A Review*. *Energy & Fuels*, 2005. **19**(5): p. 2098-2106.

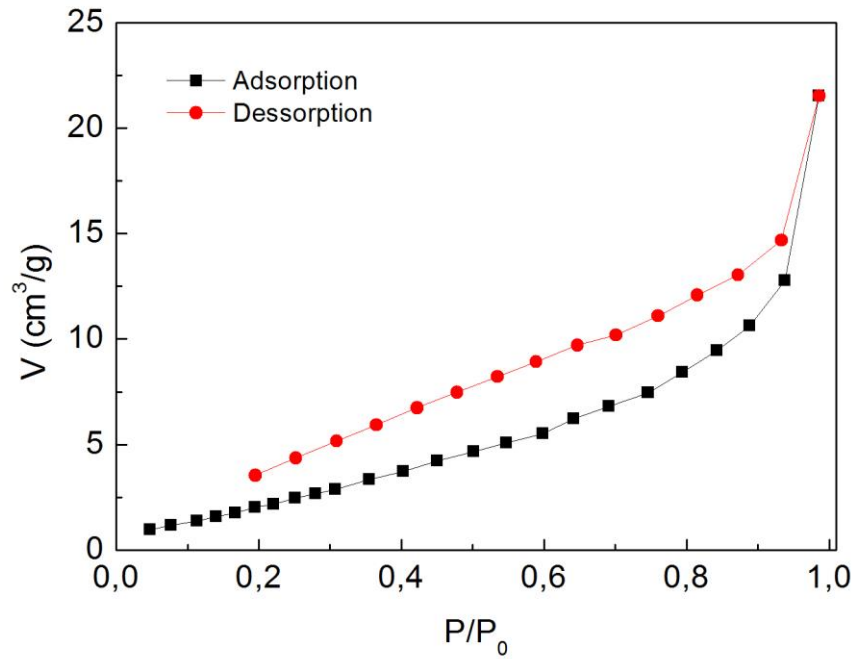
19. Holladay, J.D., et al., *An overview of hydrogen production technologies*, *Catalysis Today*. 2009. p. 244-260.
20. Braslavsky, S.E., *Glossary of terms used in photochemistry, 3rd edition (IUPAC Recommendations 2006)*. Pure and Applied Chemistry, 2007. **79**(3).
21. Wu, N., *Enhanced TiO<sub>2</sub> photocatalysis by Cu in hydrogen production from aqueous methanol solution*. *International Journal of Hydrogen Energy*, 2004. **29**: p. 1601-1605.
22. Leung, D.Y., et al., *Hydrogen production over titania-based photocatalysts*. *ChemSusChem*, 2010. **3**(6): p. 681-94.
23. Hashimoto, K., H. Irie, and A. Fujishima, *TiO<sub>2</sub> Photocatalysis: A Historical Overview and Future Prospects*. *Japanese Journal of Applied Physics*, 2005. **44**: p. 8269-8285.
24. Inagaki, M., et al., *Carbon Materials in Photocatalysis*. 2014: p. 289-311.
25. Kawai, T. and T. Sakata, *Photocatalytic Hydrogen Production from Liquid Methanol and Water*. 1980: p. 694-695.
26. Fu, X., et al., *Photocatalytic reforming of biomass: A systematic study of hydrogen evolution from glucose solution*. *International Journal of Hydrogen Energy*, 2008. **33**(22): p. 6484-6491.
27. Maeda, K., *Photocatalytic water splitting using semiconductor particles: History and recent developments*. *Journal of Photochemistry and Photobiology C: Photochemistry Reviews*, 2011. **12**: p. 237-268.
28. Silva, C.G., et al., *Influence of excitation wavelength (UV or visible light) on the photocatalytic activity of titania containing gold nanoparticles for the generation of hydrogen or oxygen from water*. *Journal of the American Chemical Society*, 2011. **133**(3): p. 595-602.
29. Chen, X., et al., *Semiconductor-based photocatalytic hydrogen generation*. *Chemical reviews*, 2010. **110**: p. 6503-70.
30. Dickinson, A., et al., *The photocatalytic reforming of methanol*. *Journal of Molecular Catalysis a-Chemical*, 1999. **146**(1-2): p. 211-221.
31. Cargnello, M. and B.T. Diroll, *Tailoring photocatalytic nanostructures for sustainable hydrogen production*. *Nanoscale*, 2014. **6**(1): p. 97-105.
32. Silva, C.G. and J.L. Faria, *Photocatalytic oxidation of phenolic compounds by using a carbon nanotube-titanium dioxide composite catalyst*. *ChemSusChem*, 2010. **3**: p. 609-18.
33. Serp, P., *Carbon nanotubes and nanofibers in catalysis*. *Applied Catalysis A: General*, 2003. **253**(2): p. 337-358.
34. Silva, C.G., W. Wang, and J.L. Faria, *Nanocrystalline CNT-TiO<sub>2</sub> Composites Produced by an Acid Catalyzed Sol-gel Method*, *Advanced Materials Forum IV*. 2008. p. 849-853.
35. Dai, K., et al., *Photocatalytic hydrogen generation using a nanocomposite of multi-walled carbon nanotubes and TiO<sub>2</sub> nanoparticles under visible light irradiation*. *Nanotechnology*, 2009. **20**(12): p. 125603.
36. Navarro, R.M., et al., *Hydrogen production from renewable sources: biomass and photocatalytic opportunities*. *Energy & Environmental Science*, 2009. **2**: p. 35.
37. Bahruji, H., et al., *Sustainable H<sub>2</sub> gas production by photocatalysis*. *Journal of Photochemistry and Photobiology A: Chemistry*, 2010. **216**(2-3): p. 115-118.
38. Bahruji, H., et al., *Sustainable H<sub>2</sub> gas production by photocatalysis*. *Journal of Photochemistry and Photobiology A: Chemistry*, 2010. **216**: p. 115-118.

39. Greaves, J., et al., *Photocatalytic methanol reforming on Au/TiO<sub>2</sub> for hydrogen production*. Gold Bulletin, 2006. **39**: p. 216-219.
40. Michael Bowker Jane Greaves, D.J.a.J.S., Lucy Millard, et al., *Photocatalysis by Au Nanoparticles: Reforming of Methanol*. Gold Bulletin, 2004. **37**: p. 170-173.
41. Al-Mazroai, L.S., et al., *The photocatalytic reforming of methanol*. Catalysis Today, 2007. **122**: p. 46-50.
42. Kondarides, D.I., et al., *Hydrogen Production by Photo-Induced Reforming of Biomass Components and Derivatives at Ambient Conditions*. Catalysis Letters. 2008. p. 26-32.
43. Sing, K.S.W., *Reporting physisorption data for gas/solid systems with special reference to the determination of surface area and porosity (Recommendations 1984)*. Pure and Applied Chemistry, 1985. **57**(4).
44. Leofanti, G., et al., *Surface area and pore texture of catalysts*. Catalysis Today, 1998. **41**(1-3): p. 207-219.
45. Silva, C.G., et al., *Developing highly active photocatalysts: Gold-loaded ZnO for solar phenol oxidation*. Journal of Catalysis, 2014. **316**: p. 182-190.

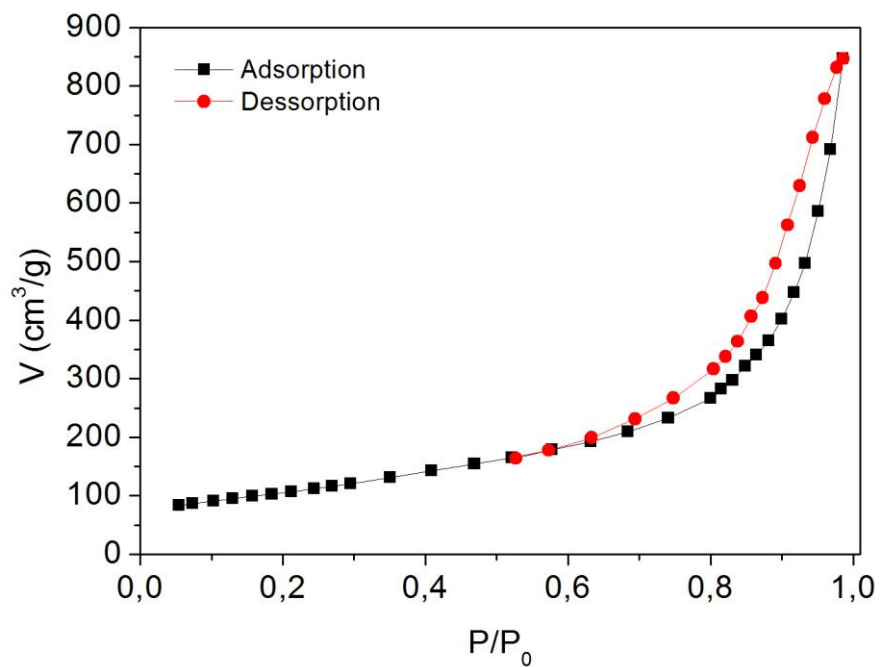


## Appendix A Characterization

a)



b)



c)

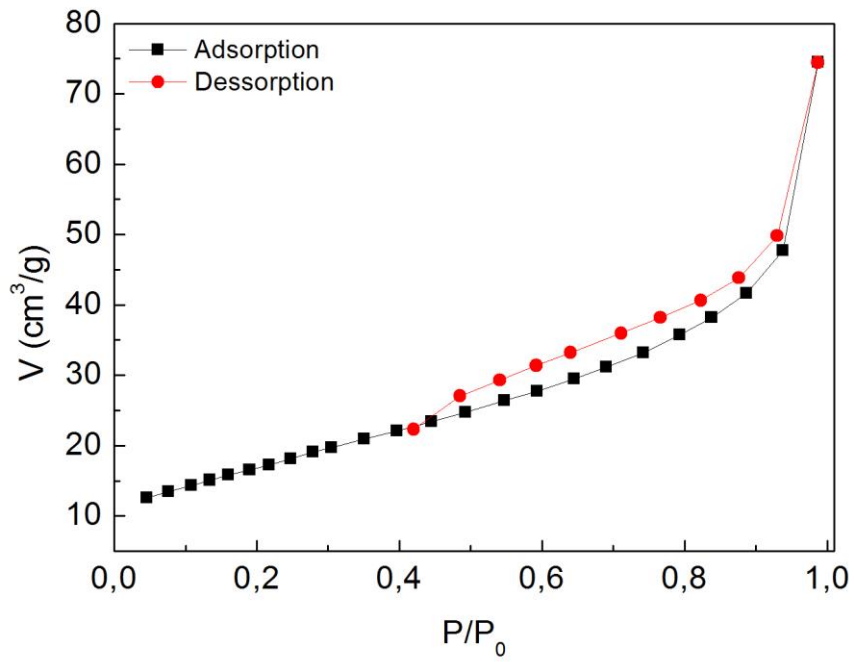


Figure 12. Isotherms for  $\text{TiO}_2$  (a), CNTs(b) and  $(\text{CNT-TiO}_2)\text{ox}$ .

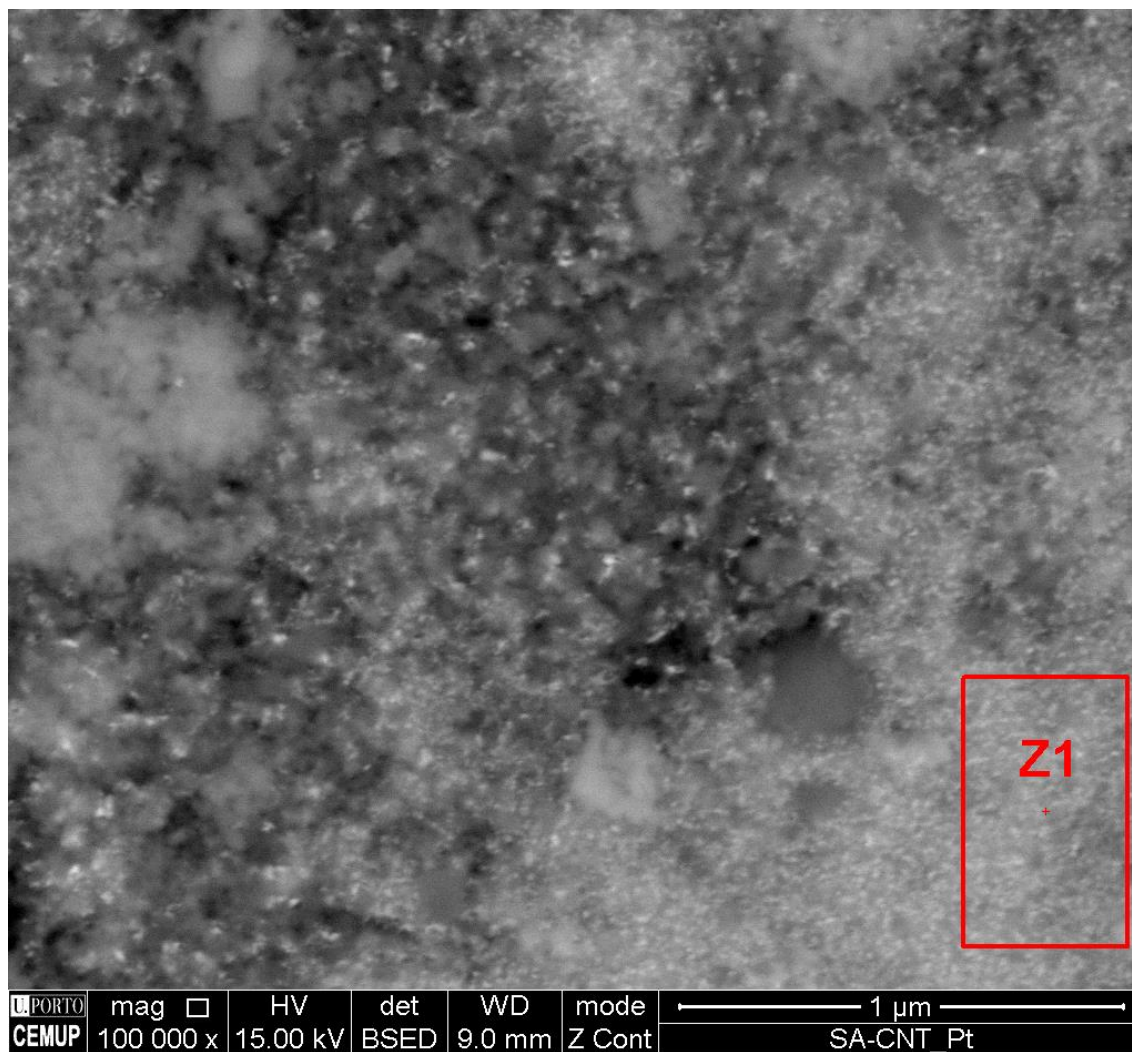
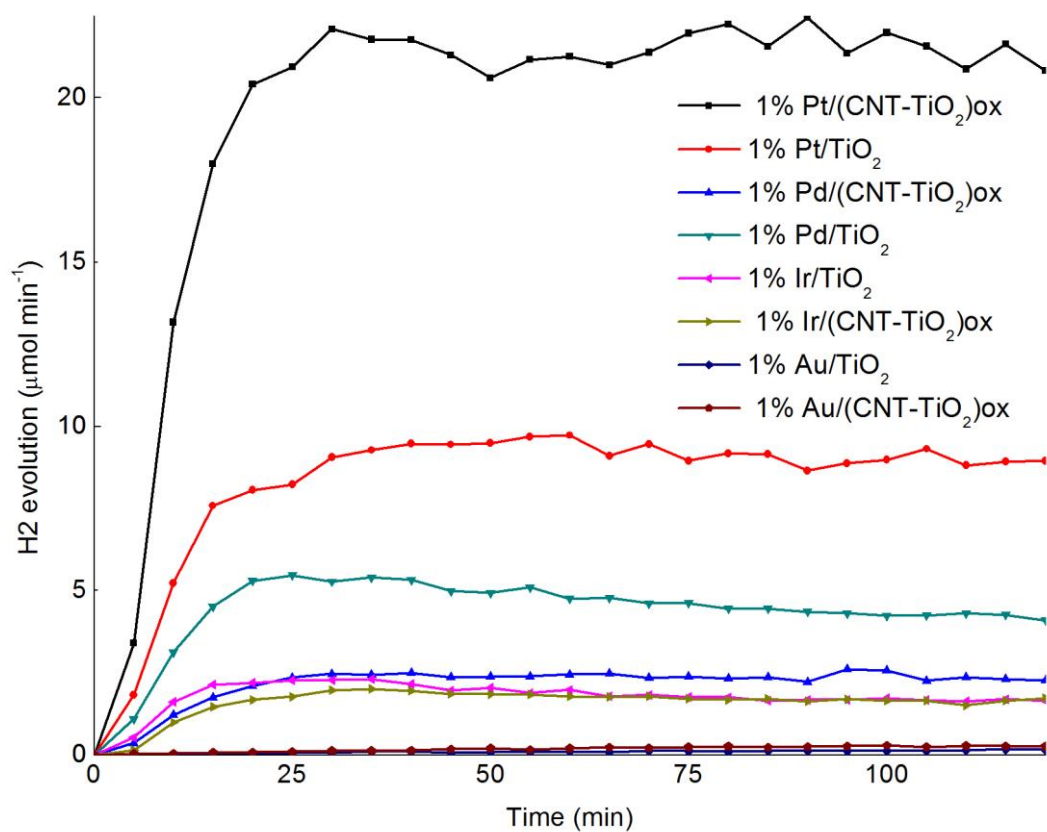


Figure 13. Z1 of 1% Pt/(CNT-TiO<sub>2</sub>)<sub>ox</sub> where was analised the EDXS spectra.

## Appendix B Results

a)



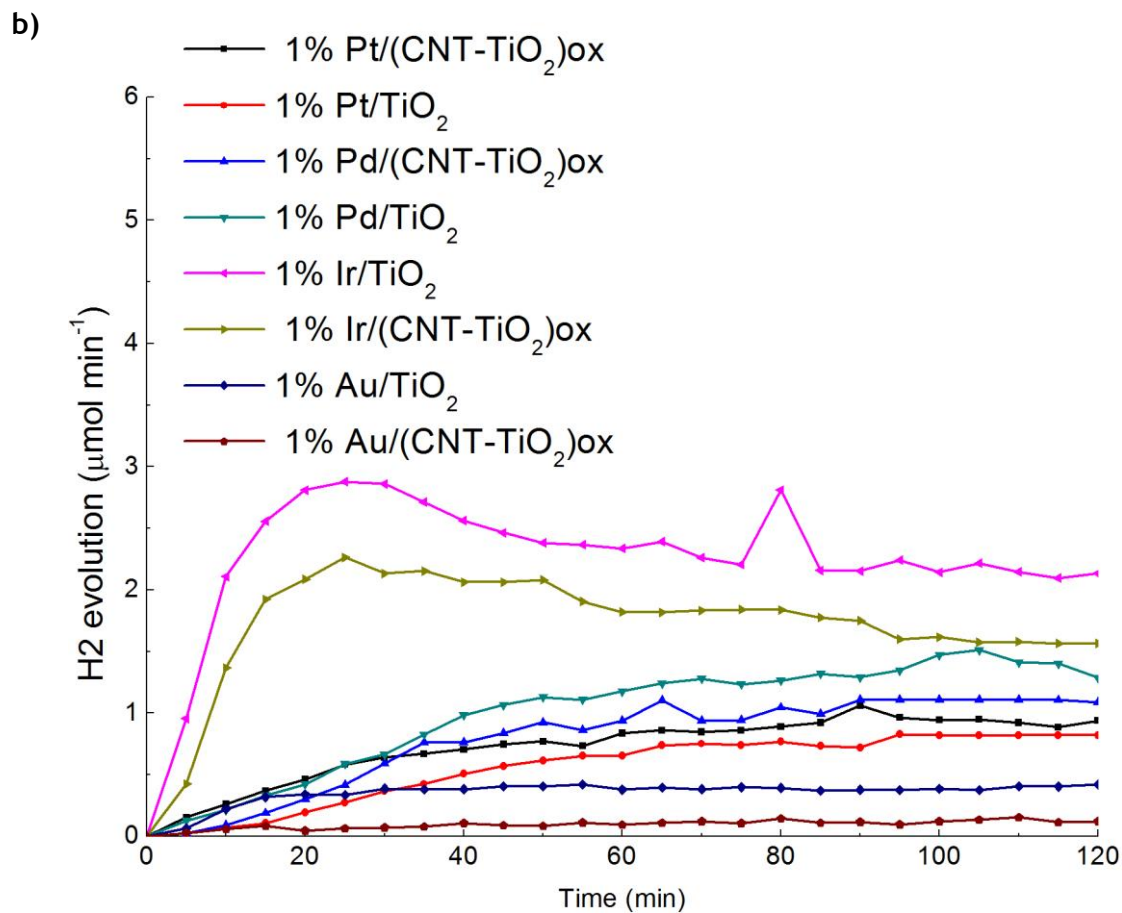


Figure 14. Evolution of hydrogen production for catalysts treated at 200 °C (a) and at 400 °C (b).